



Biogeosciences Discussions is the access reviewed discussion forum of *Biogeosciences*

BGD

2, 333–397, 2005

**A coupled model of
carbon-water
exchange of the
Amazon rain forest**

E. Simon et al.

Coupled carbon-water exchange of the Amazon rain forest, I. Model description, parameterization and sensitivity analysis

E. Simon¹, F. X. Meixner¹, L. Ganzeveld², and J. Kesselmeier¹

¹Biogeochemistry Dept., Max Planck Institute for Chemistry, Mainz, Germany

²Atmospheric Chem. Dept., Max Planck Institute for Chemistry, Mainz, Germany

Received: 24 February 2005 – Accepted: 14 March 2005 – Published: 7 April 2005

Correspondence to: E. Simon (simon@mpch-mainz.mpg.de)

© 2005 Author(s). This work is licensed under a Creative Commons License.

[Title Page](#)

[Abstract](#)

[Introduction](#)

[Conclusions](#)

[References](#)

[Tables](#)

[Figures](#)

◀

▶

◀

▶

[Back](#)

[Close](#)

[Full Screen / Esc](#)

[Print Version](#)

[Interactive Discussion](#)

EGU

Abstract

BGD

2, 333–397, 2005

Detailed one-dimensional multilayer biosphere-atmosphere models, also referred to as CANVEG models, are used for more than a decade to describe coupled water-carbon exchange between the terrestrial vegetation and the lower atmosphere. Within the 5 present study, a modified CANVEG scheme is described. A generic parameterization and characterization of biophysical properties of Amazon rain forest canopies is inferred using available field measurements of canopy structure, in-canopy profiles of horizontal wind speed and radiation, canopy albedo, soil heat flux and soil respiration, photosynthetic capacity and leaf nitrogen as well as leaf level enclosure measurements 10 made on sunlit and shaded branches of several Amazonian tree species during the wet and dry season. The sensitivity of calculated canopy energy and CO₂ fluxes to the uncertainty of individual parameter values is assessed. In the companion paper, the predicted seasonal exchange of energy, CO₂, ozone and isoprene is compared to observations.

15 A bi-modal distribution of leaf area density with a total leaf area index of 6 is inferred from several observations in Amazonia. Predicted light attenuation within the canopy agrees reasonably well with observations made at different field sites. A comparison of predicted and observed canopy albedo shows a high model sensitivity to the leaf optical parameters for near-infrared short-wave radiation (NIR). The predictions agree much 20 better with observations when the leaf reflectance and transmission coefficients for NIR are reduced by 25–40%. Available vertical distributions of photosynthetic capacity and leaf nitrogen concentration suggest a low but significant light acclimation of the rain forest canopy that scales nearly linearly with accumulated leaf area.

Evaluation of the biochemical leaf model, using the enclosure measurements, 25 showed that recommended parameter values describing the photosynthetic light response, have to be optimized. Otherwise, predicted net assimilation is overestimated by 30–50%. Two stomatal models have been tested, which apply a well established semi-empirical relationship between stomatal conductance and net assimilation. Both

A coupled model of carbon-water exchange of the Amazon rain forest

E. Simon et al.

[Title Page](#)

[Abstract](#)

[Introduction](#)

[Conclusions](#)

[References](#)

[Tables](#)

[Figures](#)

◀

▶

◀

▶

[Back](#)

[Close](#)

[Full Screen / Esc](#)

[Print Version](#)

[Interactive Discussion](#)

EGU

A coupled model of carbon-water exchange of the Amazon rain forest

E. Simon et al.

[Title Page](#)

[Abstract](#)

[Introduction](#)

[Conclusions](#)

[References](#)

[Tables](#)

[Figures](#)

[◀](#)

[▶](#)

[◀](#)

[▶](#)

[Back](#)

[Close](#)

[Full Screen / Esc](#)

[Print Version](#)

[Interactive Discussion](#)

models differ in the way they describe the influence of humidity on stomatal response. However, they show a very similar performance within the range of observed environmental conditions. The agreement between predicted and observed stomatal conductance rates is reasonable. In general, the leaf level data suggests seasonal physiological changes, which can be reproduced reasonably well by assuming increased stomatal conductance rates during the wet season, and decreased assimilation rates during the dry season.

The sensitivity of the predicted canopy fluxes of energy and CO₂ to the parameterization of canopy structure, the leaf optical parameters, and the scaling of photosynthetic parameters is relatively low (1–12%), with respect to parameter uncertainty. In contrast, modifying leaf model parameters within their uncertainty range results in much larger changes of the predicted canopy net fluxes (5–35%).

1. Introduction

Within the last decades, our understanding of atmospheric and biogeochemical processes has substantially improved. Sophisticated model schemes have been developed to describe surface exchange of trace gases and their fate in the atmosphere. For the terrestrial vegetation detailed one-dimensional multilayer biosphere-atmosphere models, also referred to as CANVEG models, are now available for more than a decade (Baldocchi, 1992; Baldocchi and Meyers, 1998). As shown in Fig. 1, these models have evolved from simple big leaf and two layer models (Deardorff, 1978; Noilhan and Planton, 1989). Although the simple models have become very useful by including detailed descriptions of soil moisture status (Dickinson et al., 1993), radiation reflectance and photosynthesis (Sellers et al., 1992, 1996) and dry deposition (Ganzeveld and Lelieveld, 1995), they are mostly empirical, which means that biophysical model parameters such as the bulk stomatal conductance have only a weak correspondence to the real world. In contrast, the CANVEG scheme integrates the exchange of trace gases and energy “bottom-up” from the leaf to the canopy level (Jarvis, 1993; Leuning

A coupled model of carbon-water exchange of the Amazon rain forest

E. Simon et al.

[Title Page](#)

[Abstract](#)

[Introduction](#)

[Conclusions](#)

[References](#)

[Tables](#)

[Figures](#)

[◀](#)

[▶](#)

[◀](#)

[▶](#)

[Back](#)

[Close](#)

[Full Screen / Esc](#)

[Print Version](#)

[Interactive Discussion](#)

et al., 1995). Therefore biophysical model parameters such as stomatal conductance correspond to biophysical leaf parameters and are calculated by a well-established mechanistic approach, which couples CO₂ exchange to transpiration and the leaf energy balance (Farquhar et al., 1980; Caemmerer and Farquhar, 1981; Ball et al., 1987; Leuning, 1990; Collatz et al., 1991; Lloyd, 1991; Collatz et al., 1992; Leuning, 1995). Most of the information required for model parameterization can be derived from eco-physiological principles, which state that photosynthetic capacity and maximum stomatal conductance are related to leaf nitrogen content, which again is determined by the light environment of the leaf and the nitrogen availability for the whole plant (Field, 1983; Hirose et al., 1988; Wullschleger, 1993; Schulze et al., 1994; Leuning et al., 1995). Furthermore, CANVEG models apply Lagrangian dispersion theory (Raupach, 1989) to calculate vertical scalar profiles within the free canopy air space. In contrast to multilayer models which apply classical K-theory, the Lagrangian approach accounts also for counter-gradient transfer and non-local dispersion across multiple layers (Raupach, 1987; Katul and Albertson, 1999; Lai et al., 2000a; Wilson et al., 2003).

Compared to a big leaf approach, the detailed description of canopy processes in CANVEG allows diagnostic applications to study feed-backs between biogeochemical and atmospheric processes (e.g. CO₂ fertilization) and to separate the influence of environmental and eco-physiological factors on trace gas exchange. Despite large data pools, being available from long-term and intensive regional studies (Grace et al., 1995; Gash et al., 1996; Sellers et al., 1997; Seufert et al., 1997; Halldin et al., 1999; Andreae et al., 2002; Gu and Baldocchi, 2002; Falge et al., 2002) for model parameterization, evaluation and application, only few vegetational types (being mainly agricultural crops, and broad-leaved and coniferous forests in temperate regions) have been investigated within a CANVEG model frame work (see Baldocchi and Harley, 1995; Baldocchi and Meyers, 1998; Baldocchi and Wilson, 2001; Lai et al., 2000a,b; Katul et al., 2003; Baldocchi and Bowling, 2003).

In the present study, we applied a modified CANVEG scheme to Amazon rain forest. Because of its large area of about $5 \times 10^6 \text{ km}^2$ (Laurance, 2000) and its all-seasonal

A coupled model of carbon-water exchange of the Amazon rain forest

E. Simon et al.

[Title Page](#)

[Abstract](#)

[Introduction](#)

[Conclusions](#)

[References](#)

[Tables](#)

[Figures](#)

[◀](#)

[▶](#)

[◀](#)

[▶](#)

[Back](#)

[Close](#)

[Full Screen / Esc](#)

[Print Version](#)

[Interactive Discussion](#)

EGU

high biological activity the Amazon rain forest plays an important role in the global climate system. Despite its vast bio-diversity, the non-flooded areas are relatively homogeneously covered by lowland deciduous tropical rain forest (“terra firma”). Since the region is located in the inner tropics, the day length, mean temperature and daily

integrated solar radiation are relatively constant. The scheme we developed is mainly a synthesis of the original CANVEG model (Baldocchi and Meyers, 1998), the Lagrangian dispersion approach proposed by Raupach (1989) and the leaf-to-canopy integration scheme described by Leuning et al. (1995). As far as we know there exist no further studies that explicitly model the coupled exchange of CO₂ and energy of Amazon rain forest canopies including the Lagrangian approach for turbulent exchange: There is the big leaf approach of Lloyd et al. (1995), focusing mainly on CO₂, and the multilayer soil-plant-atmosphere model of Williams et al. (1998), coupling the water flow from the soil to the atmosphere with C-Fixation by including a detailed soil module. However, both models differ significantly from the CANVEG type since temperature and scalar gradients inside the canopy are neglected (no transport model included). Furthermore, since those model developments many new site specific data have been provided in the meantime by LBA¹ campaigns, in our case especially by LBA-EUSTACH² in 1999 (Andreae et al., 2002).

Here we present the description of the modified CANVEG model. Using informations from LBA and Pre-LBA studies, a characterization of mean canopy structure, the distribution of photosynthetic capacity and a normalized profile horizontal wind speed is given. The subroutines to calculate the canopy radiation field and soil surface exchange as well as leaf photosynthesis and stomatal conductance, considering wet and dry season conditions, are described and evaluated. The parameterization of the Lagrangian dispersion sub-model is discussed and evaluated in detail in a further study (Simon et al., 2005b³, hereafter referred to as S2005b). Finally, the sensitivity of pre-

¹Large-Scale Biosphere-Atmosphere Experiment in Amazonia

²European Studies on Trace Gases and Atmospheric Chemistry as a Contribution to LBA

³Simon, E., Lehmann, B., Ammann, C., Ganzeveld, L., Rummel, U., Nobre, A., Araujo, A.,

dicted net fluxes to key parameter uncertainty is investigated. In a companion paper (Simon et al., 2005a), the calculated exchange of sensible and latent heat, CO₂, isoprene, and ozone as well as the vertical profiles of H₂O, CO₂ and ozone for the main research site of LBA-EUSTACH in Rondônia are compared to measurements made at two micrometeorological towers during the late wet and late dry season 1999.

2. Materials and methods

2.1. Site description and field data

Most of the data sets used in the present study were obtained at or around four micrometeorological towers installed at the two main forest research sites of LBA and the Pre-LBA study ABRACOS ⁴. The Rondônia site in southwest Amazonia is part of the Reserva Biológica Jaru (RBJ) and belongs to the Instituto Brasileiro de Meio Ambiente e Recursos Renováveis (IBAMA). It was the main forest research site of LBA-EUSTACH in 1999 (Andreae et al., 2002). There were two parts of this campaign, EUST-I and EUST-II, coinciding with the 1999 wet-to-dry (April to May) and dry-to-wet (September to November) season transition periods. The Manaus site is part of the Reserva Biológica do Cuiéiras, which belongs to the Instituto Nacional do Pesquisas da Amazônia (INPA). It is located \approx 60 km NNW of Manaus in central Amazonia and accessible by a small road. The Jaru site experiences a more marked dry season with a mean annual rainfall of 1600 mm compared to 2100 mm at the Cuiéiras site (Gash et al., 1996). Both sites can be characterized as *terra firma* with primary tropical rain forest although the dominating vegetation type differs to some extent (Grace et al., 1995; Carswell et al., 2000; Kruijt et al., 2000, S2005b).

Meixner, F., and Kesselmeier, J.: On Lagrangian dispersion of 222Rn, H₂O, and CO₂ within the Amazon rain forest, Agric. For. Meteorol., submitted, 2005b.

⁴ Anglo-Brazilian Amazonian Climate Observation Study

A coupled model of carbon-water exchange of the Amazon rain forest

E. Simon et al.

[Title Page](#)

[Abstract](#)

[Introduction](#)

[Conclusions](#)

[References](#)

[Tables](#)

[Figures](#)

◀

▶

◀

▶

[Back](#)

[Close](#)

[Full Screen / Esc](#)

[Print Version](#)

[Interactive Discussion](#)

A coupled model of carbon-water exchange of the Amazon rain forest

E. Simon et al.

[Title Page](#)

[Abstract](#)

[Introduction](#)

[Conclusions](#)

[References](#)

[Tables](#)

[Figures](#)

◀

▶

◀

▶

[Back](#)

[Close](#)

[Full Screen / Esc](#)

[Print Version](#)

[Interactive Discussion](#)

Site and tower locations are listed in Table 1. More detailed site descriptions and a general overview on LBA-EUSTACH is given by [Andreae et al. \(2002\)](#). Except the measurements of canopy structure at ZF2-C14 (which is described below), all data records used in the present study are already published and described in detail by the references given in Table 2. Therefore, we just shortly describe what this data is used for here.

Canopy structure (Λ_z) has been measured at RBJ-A, ZF2-C14, and ZF2-K34 using the optical Plant Canopy Analyzer LAI-2000 (Li-Cor, Lincoln, USA). For a comparison of different methods see [Eschenbach and Kappen \(1996\)](#). At the ZF2-C14 tower, two profiles of Λ_z have been measured on 17 July 2001 under prevailing cloudy conditions. For each profile, 12 equally distributed individual measurements were performed in a concentric circle at 4, 8, 12, 16, 20, 24, 28, 32, and 40 m height. For the further analysis using additional observations (see Table 2) the mean values from both profiles have been used. Profiles of horizontal wind speed $u(z)$ were measured at the RBJ-A tower at 1, 11, 20.7, 31.3, 42.2 and 51.7 m height ([Rummel, 2005](#)). The relationship, used to derive incoming photosynthetic active radiation (Q_{PAR}), is tested using direct observations made at RBJ-A,B and ZF2-K34. An empirical relationship to calculate incoming long-wave radiation ([Brutsaert, 1975](#)) is tested using measurements made at RBJ-B ([Andreae et al., 2002](#)). The predicted canopy albedo is compared to monthly mean values observed by [Culf et al. \(1995\)](#) and [Culf et al. \(1996\)](#) at RBJ-A and a second site near Manaus. The radiation attenuation sub-model is evaluated using: 1. Simultaneous radiation profile measurements made during ABRACOS from August to September 1992 and from April to June 1993 (six height levels at 35, 21.3, 15.7, 11.6, 6.1, 2.3 m). 2. Measurements made during EUST-II using a single sensor mounted for several days alternately at 51.7, 31.3, 20.5, and 1 m height ([Rummel, 2005](#)). 3. Mean ratios of radiation inside to above the canopy at the ZF2-C14 tower ($z=32, 28, 24, 16, 12, 8, 4$, and 0 m) in relation to values observed above the canopy as published by [Carswell et al. \(2000\)](#). From the latter study also profiles of photosynthetic capacity and leaf nitrogen concentration are available. This data is used together with leaf nitrogen

A coupled model of carbon-water exchange of the Amazon rain forest

E. Simon et al.

[Title Page](#)

[Abstract](#)

[Introduction](#)

[Conclusions](#)

[References](#)

[Tables](#)

[Figures](#)

[◀](#)

[▶](#)

[◀](#)

[▶](#)

[Back](#)

[Close](#)

[Full Screen / Esc](#)

[Print Version](#)

[Interactive Discussion](#)

EGU

concentrations measured at RBJ-A (Lloyd et al., 1995) to infer the light acclimation (i.e. the distribution of photosynthetic capacity) of the forest canopy. The parameterizations of soil respiration and soil heat flux are inferred using continuous chamber measurements and observed soil temperature and soil surface temperature gradients provided

5 by Gut et al. (2002a). The parameters for the leaf photosynthesis and stomatal models are inferred and evaluated by comparing model predictions with gas exchange measurements sampled on branches and leaves from 8 tree species growing around the tower RBJ-A. The gas exchange data for species 1–3 is obtained from two to three days of continuous cuvette measurements on tree branches and described and discussed in detail by Kuhn et al. (2002, 2004). We used hourly averages of the raw data, which has been recorded with a time resolution of 5 min. The gas exchange data for species 4–8 were measured with a portable leaf chamber by McWilliam et al. (1996) and represent mean values from three to five single leaves. All data subsets for different species, season, and canopy position have a minimum size of 10 and the total 10 number of data points is $N=498$ (183 for species 1–3).

2.2. Model description

The multilayer model has several subunits as outlined in Fig. 2. The vertical canopy column is spatially limited by the soil surface and the mean canopy height h_c . It is divided into subsequent canopy layers and a single surface layer above the canopy with

20 the upper limit z_{ref} . The scalar conservation equation is applied assuming horizontally homogeneity and steady-state environmental conditions. Vertical transport is calculated using a Lagrangian dispersion scheme (Raupach, 1989). Our implementation is described and evaluated in detail in S2005b. A short mathematical description of the integration scheme is given in Appendix 5.

25 The leaf primary exchange of CO_2 and H_2O is calculated by a combined stomatal-photosynthesis model for C_3 plants (Leuning, 1995). The coupled equations for CO_2 uptake and energy partitioning (Appendix 6) are solved numerically as described in detail by Wang and Leuning (1998). The partitioning, attenuation, and reflectance

A coupled model of carbon-water exchange of the Amazon rain forest

E. Simon et al.

[Title Page](#)

[Abstract](#)

[Introduction](#)

[Conclusions](#)

[References](#)

[Tables](#)

[Figures](#)

[◀](#)

[▶](#)

[◀](#)

[▶](#)

[Back](#)

[Close](#)

[Full Screen / Esc](#)

[Print Version](#)

[Interactive Discussion](#)

of radiation within the canopy is very complex and the most sophisticated modeling approaches require detailed informations on canopy architecture (leaf angle distribution, clumping factor, etc., see Ross, 1981). Following the scheme of Leuning et al. (1995), we included the approach of Splitters (1986), modified by Goudriaan and van Laar (1994), which accounts for the absorption and reflectance of sunlit and shaded leaves in the visible, near-infrared, long-wave radiation waveband. The non-linear light response of photosynthesis and isoprene emission justify the use of a two-stream radiation model instead of a simple extinction approach. The calculations of canopy radiation are summarized in Appendix 7.

The CANVEG model is constrained using micrometeorological parameters observed above the canopy and the temperature, water content and bulk surface conductance of the uppermost soil layer (see Table 3). For the calculation of ozone deposition, ozone background concentration observed above the canopy is included as well as input parameter. Since soil surface temperature is given as a lower boundary condition, the soil surface energy balance can be calculated straightforward as described by Garrat (1992). Soil respiration is calculated using an empirical relationship based on soil temperature (see Appendix 8 for details).

A major problem on linking biochemical leaf models to the canopy scale is the estimation and scaling of leaf physiological parameters (Jarvis, 1993). Extensive studies on nitrogen availability, allocation and optimization (Field, 1983; Field and Mooney, 1986; Walters and Field, 1987; Evans, 1989) led to the development of scaling principles for leaf physiological properties in different ecosystems and across the vertical canopy column (Wullschleger, 1993; Schulze et al., 1994; Leuning et al., 1995). Following these principles, mainly the photosynthetic capacity of sunlit leaves at the canopy top ($v_{cmax0hc}$) and the rate of acclimation to light (k_N) have to be specified for a given vegetation type. A semi-empirical relationship that couples stomatal conductance to CO_2 uptake (Ball et al., 1987) assures that maximum stomatal conductance scales indirectly with maximum photosynthesis. Therefore the stomatal model requires only few site specific informations.

2.3. Model parameterization

BGD

2, 333–397, 2005

The characterization of canopy structure represents a model key parameter. Firstly, the source/sink strength is a linear function of the leaf area of each canopy layer (Eq. 8). Secondly, it determines light extinction within the canopy and, indirectly, the scaling of leaf biochemistry (see above). Commonly, canopy structure is defined in terms of accumulated leaf area Λ_z . Denoting the mean canopy height as h_c gives $\Lambda_{hc}=0$ and $\Lambda_0 = \text{total LAI}$ (leaf area index in units of $\text{m}^2 \text{ leaf m}^{-2}$ ground). In the present study, a bi-modal vertical leaf area distribution with a lower and upper canopy maximum is assumed. This characterization is implemented as the weighted sum of two beta functions given as

$$\Lambda_z = \Lambda_0 \sum_{i=B,T} I_{x(z,i)}(a_{i1}, a_{i2}) w_i, \quad (1)$$

where $I_{x(z,i)}$ is the beta distribution function, which has limiting values $I_0=0$ and $I_1=1$ (Press, 1997). $x(z)$ represents the linearly transformed height $x=1 - z/z_i^*$ with the upper boundary z_i^* (e.g. $z_2^*=h_c$ for the distribution from the ground to the canopy top).

Each mode function has two shape parameters a_{i1} and a_{i2} and is weighted by the fractions of each distribution on total LAI (w_i). An example for Eq. (1) is given in Fig. 3a. Further ecological applications of the useful beta function are given in (Meyers and Paw U, 1986; McNaughton, 1994, S2005b).

In the next step, Λ_z is used for a vertical scaling of leaf physiological parameters. According to the light acclimation hypothesis, photosynthetic capacity of single leaves, expressed as the maximum rate of carboxylation at a reference temperature (v_{cmax0}), is co-distributed optimally with leaf nitrogen concentration (c_N), following the mean light gradients inside the canopy to maximize carbon gain (Field, 1983; Hirose et al., 1988; Leuning, 1995; Hirose and Bazzaz, 1998). Up to now, only a few observations of the degree of light acclimation in natural canopies exist (e.g. in Meir et al., 2002). Assuming a linear relationship between v_{cmax0} and c_N , Leuning et al. (1995) proposed

$$v_{cmax0}(\Lambda_z) = v_{cmax0hc} \exp(-k_N \Lambda_z), \quad (2)$$

A coupled model of carbon-water exchange of the Amazon rain forest

E. Simon et al.

[Title Page](#)

[Abstract](#)

[Introduction](#)

[Conclusions](#)

[References](#)

[Tables](#)

[Figures](#)

[◀](#)

[▶](#)

[◀](#)

[▶](#)

[Back](#)

[Close](#)

[Full Screen / Esc](#)

[Print Version](#)

[Interactive Discussion](#)

EGU

A coupled model of carbon-water exchange of the Amazon rain forest

E. Simon et al.

where k_N is an extinction coefficient specifying the degree of acclimation and $v_{cmax0hc}$ the value of v_{cmax0} at the canopy top. For illustration, Eq. (2) is applied using different values for k_N for a given canopy structure (Fig. 3b). A high value of k_N is associated with a strong decrease of v_{cmax0} . $v_{cmax0hc}$ can be estimated from ecological databases of nitrogen availability. For tropical rain forest, a low nitrogen availability can be assumed (Schulze et al., 1994) predicting a value of $50 \mu\text{mol m}^{-2} \text{ s}^{-1}$. The remaining parameters of the leaf models are set to the values listed in Table 7. In Sect. 3.4, the value of $v_{cmax0hc} = 50 \mu\text{mol m}^{-2} \text{ s}^{-1}$ is evaluated and k_N is inferred.

The calculation of the leaf boundary-layer resistance (see Appendix 6) requires a parameterization of the profile of horizontal wind speed $u(z)$. We use a slightly modified version of the combined approach of Kaimal and Finnigan (1994), applying a logarithmic decrease above and an exponential decrease below the canopy height (h_c) according to

$$u(z) = \begin{cases} u_{ref} a_u \ln \left(\frac{z-d_h}{z_0} \right); & z \geq h_c \\ u_0 + u(h_c) \exp \left[-k_u \Lambda_0 (1 - z/h_c) \right]; & \text{else} \end{cases}, \quad (3)$$

where a_u and k_u are two empirical coefficients, and z_0 , and d_h the roughness length and the displacement height below h_c , respectively (see Fig. 3c for an example). The offset function $u_0(z)$ is introduced to account for the fraction of $u(z)$ that does not scale with u_{ref} . Parameter values are derived from profile measurements by fitting the logarithmic and exponential functions to measurements made above and below h_c , respectively.

Atmospheric emissivity (ϵ_{a0}) is required to calculate the incoming long-wave radiation and derived using the empirical relationship of Brutsaert (1975) giving

$$\epsilon_{a0} = 1.24 \left(\frac{e_{ref}}{T_{ref}} \right)^{1/7}, \quad (4)$$

where e_{ref} and T_{ref} are the water vapor pressure (hPa) and temperature (K) above the canopy. According to Jones (1992), the visible (Q_{V0}) and photosynthetic active

Title Page

Abstract

Introduction

Conclusions

References

Tables

Figures

◀

▶

◀

▶

Back

Close

Full Screen / Esc

Print Version

Interactive Discussion

radiation (Q_{PAR} in units of $\mu\text{mol m}^{-2} \text{ s}^{-1}$) can be calculated from the incoming global radiation ($gRad$) as

$$Q_{V0} = 0.45gRad \quad (5)$$

$$Q_{PAR} = 4.5\mu\text{mol J}^{-1} Q_V. \quad (6)$$

5 The soil heat flux is calculated by solving the Penman-Monteith equation for the pathway from the soil surface to the ambient air layer above. The bulk soil surface conductance for heat is derived from observed soil heat fluxes and temperature gradients. Soil evaporation and respiration are calculated as described in Appendix 8. The Arrhenius curve to predict soil respiration is derived from observations from soil chamber measurements. The parameterization of soil evaporation (see Appendix 8) is not evaluated independently here, since appropriate data sets are missing. Jones (1992) estimates that E_{soil} is usually less than 5% of the total evapotranspiration for canopies with a total LAI of 4 and more, even when the soil surface is wet.

10

3. Results and discussion

15 In the following sections, the data sets listed in Table 2 are used to characterize the rain forest canopy (canopy structure, extinction profile of horizontal wind speed, canopy albedo, canopy biochemistry) and to derive or evaluate important model parameter values (number of model layers, bulk soil surface conductance). The leaf models for photosynthesis and stomatal conductance are evaluated with scale appropriate data (leaf chamber and cuvette measurements) and the sensitivity of predicted canopy net fluxes of CO_2 and energy is assessed with respect to the uncertainties of key parameters derived before.

20

BGD

2, 333–397, 2005

A coupled model of carbon-water exchange of the Amazon rain forest

E. Simon et al.

[Title Page](#)

[Abstract](#)

[Introduction](#)

[Conclusions](#)

[References](#)

[Tables](#)

[Figures](#)

◀

▶

◀

▶

[Back](#)

[Close](#)

[Full Screen / Esc](#)

[Print Version](#)

[Interactive Discussion](#)

EGU

3.1. Characterization of canopy structure

BGD

2, 333–397, 2005

All available measurements of canopy structure listed in Table 2 are fitted to Eq. (1). Considering literature data and ecological principles, we assume a lower and upper leaf area density maximum at 0–5 and 15–30 m height, reflecting the ground vegetation and small trees in the lower canopy and tall trees, lianes, and epiphyta in the upper canopy, respectively. The upper canopy height is estimated as $h_c=40$ m (see Klinge et al., 1975; McWilliam et al., 1993; Roberts et al., 1993; Kruyt et al., 2000; Andreae et al., 2002; Rummel et al., 2002, S2005b). All observations listed in Table 2 are averaged for 3 m height intervals. Equation (1) is then fitted to the mean values assuming I_B and I_T as the beta functions representing the lower and upper maximum of the leaf area distribution, respectively. Total LAI is set to $\Lambda_0=6$, representing the mean value of all measurements. Weights and upper bounds are estimated as $w_B=0.25$, $w_T=0.75$ and $z_B^*=13$ m, $z_T^*=h_c$ (40 m). Local optimization of the coefficients a_{i1} and a_{i2} leads to the parameter values listed in Table 4, including estimates for a “dense forest type” with higher leaf area densities in the upper canopy (LAI=6.5) and for an “open forest type” with higher densities near the ground (LAI=5.5). The scatter plot (Fig. 4a) and the mean vertical profiles (Fig. 4b) show a good agreement between measurements and predictions ($r^2=0.95$). The modifications for dense and open forest types are derived from the standard deviations of mean values. The mean differential profile ($d\Lambda_z$ for 3 m height intervals, see Fig. 4c) is scattered but shows clearly two different modes.

The characterization described above may be helpful for future modeling studies where a definition of canopy structure is required. Variations of the vegetation type may be considered by modifying the parameters values listed in Table 4.

3.2. Horizontal wind speed

The parameters of the function describing the profile of horizontal wind speed $u(z)$ have been derived using observations at the Jaru site (Table 2). The measurements suggest a significant positive intercept u_0 , which decreases with height according to $u_0(z)=0.1$

A coupled model of carbon-water exchange of the Amazon rain forest

E. Simon et al.

[Title Page](#)

[Abstract](#)

[Introduction](#)

[Conclusions](#)

[References](#)

[Tables](#)

[Figures](#)

[◀](#)

[▶](#)

[◀](#)

[▶](#)

[Back](#)

[Close](#)

[Full Screen / Esc](#)

[Print Version](#)

[Interactive Discussion](#)

EGU

$m\ s^{-1}$, $z \leq d_h$ and $u_0(z)=0.1[1-(z-d_h)/(z_{ref}-d_h)]$, $z>d_h$. The logarithmic part of Eq. (3) is derived by a non-linear fit, resulting in $z_0=1.3\ m$, $d_h=29\ m$ and $a_{u1}=1/3$. Linear-fitting of the exponential part of Eq. (3) predicts an extinction coefficient $k_u=0.8$. The linear correlation between all measurements and the parameterization is $r^2=0.94$ showing no systematic deviations.

3.3. Radiation

The empirical relationship between atmospheric emissivity (ϵ_{a0}) and water vapor pressure and temperature (T_{ref} , Eq. 4) is evaluated by a comparison of simulated and observed ϵ_{a0} and incoming long-wave radiation ($Q_{LW\downarrow}$) measured at the RBJ-B tower (Fig. 5). For high emissivity values ($\epsilon_{a0}>0.9$), the parameterization shows a systematic error of 1–10%, resulting in an underestimation of $10\text{--}20\ W\ m^{-2}$ for $Q_{LW\downarrow}$ at noon time. However, this is less than 5% on relative terms since $Q_{LW\downarrow}$ is mainly determined by T_{ref} .

The number (n) and thickness (Δ_z) of canopy layers are parameters that determine model accuracy and numerical stability. To infer the sensitivity of predicted absorbed radiation in relation to the number of model layers, we assumed a canopy with black leaves (no albedo!). As shown in Fig. 6a, the relative error of predicted absorbed radiation (Q_{abs}) increases linearly from 1% for $n=13$ ($\Delta z=3\ m$) to 9% for $n=3$ ($\Delta z=13.3\ m$). As a good compromise between prediction error and computational costs, a number of $n=8$ canopy layers is derived. In fact this meets the accuracy criteria of Norman and Welles (1983) closely, recommending a maximum leaf area of 0.5 for a given model layer. For an open canopy, predicted absorbed radiation is also dependent on LAI (Fig. 6b). However, for $LAI \geq 4$, the soil absorbs only little energy while more than 90% of incoming short-wave radiation is absorbed by leaves. This implies a low sensitivity of predicted canopy net fluxes in relation to the uncertainty of LAI. This point is discussed in more detail in Sect. 3.7.

Since leaves are usually not black, incident radiation is partially reflected and transmitted, which is considered by two model parameters, the leaf scattering (σ_l) and the

BGD

2, 333–397, 2005

A coupled model of carbon-water exchange of the Amazon rain forest

E. Simon et al.

[Title Page](#)

[Abstract](#)

[Introduction](#)

[Conclusions](#)

[References](#)

[Tables](#)

[Figures](#)

◀

▶

◀

▶

[Back](#)

[Close](#)

[Full Screen / Esc](#)

[Print Version](#)

[Interactive Discussion](#)

EGU

A coupled model of carbon-water exchange of the Amazon rain forest

E. Simon et al.

[Title Page](#)

[Abstract](#)

[Introduction](#)

[Conclusions](#)

[References](#)

[Tables](#)

[Figures](#)

[◀](#)

[▶](#)

[◀](#)

[▶](#)

[Back](#)

[Close](#)

[Full Screen / Esc](#)

[Print Version](#)

[Interactive Discussion](#)

canopy reflection (ρ_c) coefficients, respectively. In Fig. 7, the predicted canopy albedo for clear sky conditions at midday is compared to longterm observations made by Culf et al. (1995) and Culf et al. (1996) at the Jaru site and at a second site near Manaus. Using the recommended values for σ_i and ρ_c , the predicted albedo of 23.2% is nearly double as high as the observed values of 12–14%. Since radiation absorption is maximal in the visible range, the predicted albedo is much more sensitive to the selection of σ_{IN} and ρ_{cN} , the scattering and reflection coefficients for near-infrared radiation, respectively (Fig. 7a). Reducing the scattering and reflection of visible radiation from 100 to 0% (from 0.2 and 0.057 to 0 for σ_{IV} and ρ_{cdV} , respectively) results in a small reduction of canopy albedo ($\approx 2.1\%$) whereas the same scaling for near-infrared radiation (from 0.8 and 0.389 to 0 for σ_{IN} and ρ_{cdN} , respectively) reduces the albedo essentially from 23.2 to 4.3%. To minimize the large disagreement between observed and predicted canopy albedo, we have scaled leaf optical properties as listed in Table 5, although this selection cannot be validated. However, these findings are in agreement with the results of Wang (2003), who showed that the radiation model of Goudriaan and van Laar (1994) generally underestimates the amount of absorbed radiation. One further explanation for the poor agreement, which is obtained with non-optimized parameter values could be the model assumption of a spherical leaf angle distribution, which is probably not fulfilled in forest ecosystems (Ross, 1981). Furthermore, in natural ecosystems, the orientation of leaves may change during the day (Jones, 1992) and optimize the ratio of absorbed to reflected canopy radiation. We assessed the significance of the parameter modifications for the CANVEG scheme in Sect. 3.7.

Equations (5–6) imply the relationship $Q_{PAR0}=2.025 \mu\text{mol J}^{-1} g\text{Rad}$ which was tested by comparing measured and predicted values for a one month period (Jaru towers and ZF2-K34). As shown in Fig. 8a, the observations show an excellent fit to the relationship ($r^2=1.00$).

The radiation model is tested further by comparing the mean observed and predicted mean ratios $Q_{PAR}(\Lambda_z)/Q_{PAR0}$ at different canopy positions Λ_z (Fig. 8b). Model results are calculated using input data from RBJ-A tower in October 1999. $Q_{PAR}(\Lambda_z)/Q_{PAR0}$

A coupled model of carbon-water exchange of the Amazon rain forest

E. Simon et al.

is derived from the weighted sums of photosynthetic active radiation absorbed by the sunlit and shaded leaf area of a layer divided by incoming Q_{PAR0} above the canopy. A simple log-linear fit is also shown. In general, all measurements show a similar light attenuation at lower canopy positions $\Lambda_z > 4$. Compared to observations, the two-stream radiation model predicts a lower ratio near the canopy top and a higher ratio at $\Lambda_z \geq 4$. Nevertheless, the agreement is reasonable considering the measurement uncertainties in Λ_z and $Q_{PAR}(z)$. The simple log-linear model predicts an optimal extinction coefficient of 0.82, which is close to the extinction coefficient for diffuse radiation and black leaves $k_d^B = 0.8$ (see [Leuning et al., 1995](#)). Summarizing, the results support the assumption, that the investigated sites have a comparable canopy structure and radiation field, which can be calculated reasonably well by the two-stream radiation sub-model.

3.4. Light acclimation of photosynthetic capacity

A linear $v_{cmax} - c_N$ relationship, expressed on leaf area basis, and an exponential decrease with accumulated leaf area Λ_z is applied (Eq. 2) to characterize biochemical properties of the rain forest canopy relevant for CO_2 and H_2O exchange (see Sect. 2.3). In Fig. 9a, v_{cmax0} observed by [Carswell et al. \(2000\)](#) at ZF2-C14 is plotted against Λ_z measured at the same tower (see Table 2). The observed light acclimation ($k_N = 0.2$) predicts a 70% reduction of v_{cmax0} for ground vegetation ($\text{LAI} = 6$) and agrees with the shape of leaf nitrogen distribution observed by [Lloyd et al. \(1995\)](#) at the RBJ-B tower (Fig. 9b), averaged for 6 height classes (0–2, 9–12, 13–15, 16–21, 22–26, and 27–30 m). The correlation between v_{cmax0} and Λ_z is nearly linear ($r^2 = 0.9$). Extrapolation of the straight fitted line to the canopy top predicts $v_{cmax0hc} \approx 50 \mu\text{mol m}^{-2} \text{ s}^{-1}$, which is identical to the value for tropical rain forest estimated by [Wullschleger \(1993\)](#) and the value for low nitrogen plants estimated by [Leuning et al. \(1995\)](#). Although the relationship between leaf nitrogen concentration and maximum carboxylation rate may also be expressed on a leaf mass basis ([Schulze et al., 1994](#); [Meir et al., 2002](#)), especially when different ecosystems are compared, the relationship based on leaf area seems to be more appropriate for leaf-to-canopy scaling ([Hirose and Werger, 1987](#); [Leuning](#)

Title Page

Abstract

Introduction

Conclusions

References

Tables

Figures

◀

▶

◀

▶

Back

Close

Full Screen / Esc

Print Version

Interactive Discussion

3.5. Soil surface exchange

Measured soil heat flux (G) and temperature gradients between -0.05 m soil depth and

5 1 m height above the ground are used to derive the bulk soil surface conductance for
heat (g_{soilH} , RBJ-A tower, see Table 2). As shown in Figs. 10a–b, the assumption of a
constant bulk conductance $1/g_{soilH}=500$ s m $^{-1}$ gives an excellent model fit ($r^2 = 0.92$).
Typically for dense forest canopies, G is relatively small (<15 W m $^{-2}$). Figure 10a shows
10 a comparison of measurements and predictions for a limited period in the late dry
season. Obviously, the parameterization can explain most of the observed variations
of G .

The empirical relationship between soil respiration (F_{csoil}) and temperature (Eq. 36)
is assessed using continuous measurements from 3 soil chambers made by Gut et al.
(2002a) in October and November 1999 at the Jaru site. Figure 10c shows the mean
15 values and standard deviations of F_{csoil} determined for 0.5°C intervals. For a reference
temperature of 25°C, a respiration of $F_{csoil0}=3.3$ $\mu\text{mol m}^{-2} \text{s}^{-1}$ is derived, which is
close to the mean value of 3.13 ± 1.3 $\mu\text{mol m}^{-2} \text{s}^{-1}$ (mean soil temperature is 24.5°C).
The frequency distribution of F_{csoil} has a single mode (Fig. 10d). A plot of mean values
20 against temperature intervals for classes with more than $N = 10$ observations (Fig. 10c)
shows a slight exponential increase within the narrow temperature range (4°). The
optimal fit of Eq. (36) is close to the model derived by Meir et al. (1996) for another site
in Amazonia and predicts a realistic Q_{10} value of 1.5–2.3 (Q_{10} describes the relative
increase rate of a biological process for a temperature increase of 10°C). Considering
25 these results, reference soil respiration and activation energy are $F_{csoil0}=3.3$ $\mu\text{mol m}^{-2}$
 s^{-1} and $H_{asoil}=60$ kJ mol $^{-1}$, respectively (see Appendix 8).

A coupled model of carbon-water exchange of the Amazon rain forest

E. Simon et al.

[Title Page](#)

[Abstract](#)

[Introduction](#)

[Conclusions](#)

[References](#)

[Tables](#)

[Figures](#)

◀

▶

◀

▶

[Back](#)

[Close](#)

[Full Screen / Esc](#)

[Print Version](#)

[Interactive Discussion](#)

Leaf level gas exchange measurements from 8 Amazonian tree species are used to evaluate the photosynthesis and stomatal conductance models described in Sect. 2.2 and Appendix 6. Three seasonal periods are considered (late wet, early dry, and late dry season). The photosynthesis model is constrained using measurements of leaf temperature, incident PAR outside the leaf chamber (Q_{PAR}), and intercellular carbon dioxide concentration, calculated according to Ball (1987). The absorbed PAR radiation (Q_{abs}) is calculated as a fixed fraction of Q_{PAR} assuming $Q_{abs}=0.9Q_{PAR}$. Vertical canopy position is estimated by combining Λ_z observed at RBJ-A (see Sect. 3.1) with observed mean ratios $Q_{PAR}(\Lambda_z)/Q_{PAR0}$ (species 1–3, see Fig. 8b) or, if branch height was available, directly with z (4–8). The sub-models are calibrated with recommended parameter values as listed in Table 7. Maximum carboxylation rates (v_{cmax0}) and related parameters are scaled according to Eq. (2) using $k_N=0.2$ (Fig. 11a, see also Sect. 3.4). The reference leaf temperature for kinetic parameters is adopted from the common value of 20°C (Harley et al., 1992; Leuning, 1995) to 25°C for tropical species (Carswell et al., 2000; Lloyd et al., 1995). Predicted optimum leaf temperature for v_{cmax} and the maximum rate of electron transport (J_{max}) are 40.2 and 34.4°C, respectively.

A comparison of the observed and predicted photosynthesis rates for late wet, early dry and late dry season conditions is shown in Figs. 12a–f. Using recommended parameter values to describe the light response and shape of the temperature dependence for the photosynthesis model leads to a large overestimation of observed A_n . The observations show a lower light use efficiency (α), indicated by the lower initial slope of the light response curve. Furthermore, net assimilation rates at saturating irradiance above 800 $\mu\text{mol m}^{-2} \text{s}^{-1}$ are overestimated by 30–70%. The measurements exhibit even a decline of A_n at very high irradiance as observed especially for late dry season conditions. By decreasing α from 0.2 to 0.15 and the optimum leaf temperature for J_{max} from 34.4 to 326°C, the model performs much better, indicated by the slope and intercept of the linear fits (Figs. 12d–f). For the dry season data sets of species 1

A coupled model of carbon-water exchange of the Amazon rain forest

E. Simon et al.

[Title Page](#)

[Abstract](#)

[Introduction](#)

[Conclusions](#)

[References](#)

[Tables](#)

[Figures](#)

◀

▶

◀

▶

[Back](#)

[Close](#)

[Full Screen / Esc](#)

[Print Version](#)

[Interactive Discussion](#)

and 4, the offset value is $\approx 7 \mu\text{mol m}^{-2}\text{s}^{-1}$ (not shown here). Obviously, photosynthesis of single species is reduced during the dry season suggesting a seasonal change of leaf physiological parameters.

Taking the measurement uncertainties and the large seasonal and species dependent variability into consideration, the model results agree reasonably well with the observations. However, the results demonstrate the high sensitivity of model predictions to the choice of individual parameter values. The optimized photosynthesis parameters are listed in Table 7.

The two stomatal models of [Ball et al. \(1987\)](#) and [Leuning et al. \(1995\)](#), hereafter referred to as B87 and L95, respectively (see Appendix 6), are very similar. For comparison, B87 and L95 are constrained using observed A_n , relative humidity h_s (only B87) or water pressure deficit D_s (only L95) and concentration of CO_2 at the leaf surface c_s , assuming a fixed CO_2 compensation point ($\Gamma^* = 38.5 \mu\text{mol mol}^{-1}$). The empirical parameter expressing the sensitivity of stomatas to D_s , D_{s0} , is set to 15 hPa (only L95), the minimum stomatal conductance and the empirical coefficient relating g_s to A_n are set to $g_{s0} = 0.01 \text{ mol m}^{-2} \text{ s}^{-1}$ ([Leuning, 1995](#)) and $a_A = 10$ ([Ball et al., 1987](#); [Harley et al., 1992](#)), respectively. Since not all constraining parameters are available for the data of [McWilliam et al. \(1996\)](#), the analysis of g_s is restricted to the first three species listed in Fig. 11 ($N = 183$). A comparison of model predictions and observations is shown Fig. 13.

Both models fail to predict considerable variability observed with g_s . However, systematic deviations are small taking into consideration that model parameters (g_{s0} , a_A and D_{s0}) have not been optimized locally. The relatively poor fit for both stomatal models is to some extent in agreement with the results of [Lloyd et al. \(1995\)](#) who also evaluated the more detailed but purely empirical approach of [Jarvis \(1976\)](#), which requires many additional parameters that are usually not available. In contrast, the simple B87 and L95 models apply a simple but robust relationship between g_s and A_n , which seems to be a reasonable description of stomatal behavior over a wide range of environmental and ecophysiological conditions.

A coupled model of carbon-water exchange of the Amazon rain forest

E. Simon et al.

[Title Page](#)

[Abstract](#)

[Introduction](#)

[Conclusions](#)

[References](#)

[Tables](#)

[Figures](#)

◀

▶

◀

▶

[Back](#)

[Close](#)

[Full Screen / Esc](#)

[Print Version](#)

[Interactive Discussion](#)

3.7. Model sensitivity to key parameter uncertainty

BGD

2, 333–397, 2005

A coupled model of carbon-water exchange of the Amazon rain forest

E. Simon et al.

[Title Page](#)

[Abstract](#)

[Introduction](#)

[Conclusions](#)

[References](#)

[Tables](#)

[Figures](#)

[◀](#)

[▶](#)

[◀](#)

[▶](#)

[Back](#)

[Close](#)

[Full Screen / Esc](#)

[Print Version](#)

[Interactive Discussion](#)

EGU

In the following section, the sensitivity of predicted canopy net fluxes (energy and CO₂) to the inferred parameter uncertainties (Sects. 3.1–3.6) is assessed. These parameters include canopy structure, the scaling of albedo parameters (leaf transmittance σ , and reflectance ρ_c for visible and near-infrared radiation, respectively), the photosynthetic capacity of canopy top leaves ($v_{cmax0hc}$) and the distributing of leaf nitrogen (light acclimation coefficient k_N). Additionally, seasonal changes in leaf physiology are considered by applying a model parameterization with higher stomatal conductances for wet season conditions and lower assimilation rates for dry season conditions: For wet season conditions, the parameter correlating stomatal conductance with assimilation (a_A) is increased from 10 to 15 (see also Lloyd et al., 1995). For dry season conditions, the light use efficiency (α , the initial slope of light response), is reduced from 0.15 to 0.1 and the shape parameter of the hyperbolic light response function (θ) is reduced from the recommended value of 0.9 to 0.8. Table 6 compiles the derived model parameters and the applied uncertainty range for calculating the sensitivities of canopy fluxes of sensible heat (H), latent heat (LE) and CO₂ (NEE), predicted by the CANVEG model. The model is constrained using mean diurnal cycles of meteorological variables (Table 3) observed during the late wet and late dry season at the RBJ-A tower in Jaru in 1999. The input data is described in more detail in the companion paper (Simon et al., 2005a). The flux sensitivities as listed in Table 6 (last three columns on the right) are derived by relating the model output, obtained by modifying a single parameter (second column on the left) while keeping all others constant, to the model output obtained with the reference parameterization, inferred in Sects. 3.1–3.6 (left column). Most relationships are nearly linear within the parameter range inferred. The parameters of the photosynthesis model have been assessed in parallel (5th and 6th line in Table 6).

For canopy structure, a relatively low sensitivity of model predicted net fluxes is found. The largest variability is found for the sensible heat flux, which decreases by 12% for the open canopy compared to the dense canopy type. This may be partly

explained by increased albedo (5%) and net radiation (3%) For the open canopy type, net assimilation is reduced by 5%, whereas it is increased by 2% for the dense type. This is quite consistent with the derived relationship between LAI and absorbed short wave radiation (Q_{abs}), which predicts a saturation of Q_{abs} at $LAI \geq 4$ (Sect. 2.3).

As discussed in Sect. 3.3, the recommended parameter values for leaf optical parameters predict a much higher canopy albedo as observed. The best fit to measurements is obtained when σ_l and ρ_c are scaled down to 60–75% of the recommended values. However, the model predicted energy fluxes are not very sensitive to the uncertainty of these parameters. The 20% variability in canopy albedo results in less than 5% variability in predicted H and LE . Surprisingly, the sensitivity of canopy net assimilation to the photosynthetic capacity at the canopy top is relatively low (Fig. 14e,f). Increasing $\nu_{cmax0hc}$ by 40% increases the net CO_2 uptake by only 5%. For LE , these differences are even smaller. Obviously, the contribution of lower canopy layers to the total exchange of LE and NEE is low and increasing respiration of the whole foliage compensates the effect of increasing gross assimilation. The second important parameter related to canopy biochemistry is k_N , representing the extinction coefficient of photosynthetic capacity (zero value means no acclimation). In Sect. 2.3, an optimal value of 0.2 has been inferred. The flux sensitivities listed in Table 6 indicate nearly optimal distribution of leaf nitrogen since NEE remains constant with decreased k_N (which increases ν_{cmax0} in the lower canopy). In contrast, increasing k_N leads to a significant reduction of CO_2 uptake (35%).

Compared to the results described above, the predicted fluxes are much more sensitive to the physiological parameters (lines 5–7 in Table 6). Figure 14 shows the results in more detail. The energy fluxes (H and LE) and bowen ratios (H/LE) are very sensitive to the stomatal parameter (a_A), whereas net assimilation is most sensitive to the leaf photosynthesis parameters (α, θ). Reducing a_A from 10 to 5 results in a 41% reduction of LE and a 25% increase of H whereas net assimilation is reduced by 22%. Increasing a_A from 10 to 15 results in a 22% increase of LE and a 22% decrease of H . Increasing the photosynthetic parameters ($\alpha=0.2, \theta=0.95$) leads to a nearly lin-

A coupled model of carbon-water exchange of the Amazon rain forest

E. Simon et al.

[Title Page](#)

[Abstract](#)

[Introduction](#)

[Conclusions](#)

[References](#)

[Tables](#)

[Figures](#)

◀

▶

◀

▶

[Back](#)

[Close](#)

[Full Screen / Esc](#)

[Print Version](#)

[Interactive Discussion](#)

ear increase of NEE and LE (26% and 114%, respectively), whereas H is decreased by 5%. In the opposite direction, the effect of parameter modification is even larger. Reducing the photosynthesis parameter ($\alpha=0.1$, $\theta=0.8$), results in a 34% reduction of NEE. Since CO_2 is coupled to the water exchange, the partitioning of energy is also effected resulting in a strong decrease of LE (22%) and increase (11%) of sensible energy. These results stress the necessity of careful parameter selection and sub-model evaluation with scale appropriate data (Sect. 3.6)

4. Conclusions

An integrated CANVEG model scheme, describing the coupled exchange of carbon and energy between the Amazon rain forest and the lower atmosphere, has been presented.

- The evaluation of calculations related to leaf photosynthesis using scale appropriate cuvette measurements made on branches and leaves of 8 tree species at different canopy positions during three seasonal periods, showed a reasonable agreement between model predictions and observations after optimization of recommended parameter values for the temperature optimum of the electron transport rate (decreased), light use efficiency (decreased), and the shape parameter describing the transition from linear to saturated light response (increased).
- The branch-level measurements indicate also a seasonal variability of leaf physiology. This is investigated in more detail within the companion paper by applying different parameterization schemes, that assume increased stomatal conductance rates for wet season conditions (by increasing the stomatal parameter a_A from 0.15 to 0.2) and decreased photosynthesis rates for dry season conditions (by decreasing the light-use-efficiency α from 0.15 to 0.1 and the rectangular shape parameter θ from 0.9 to 0.8, respectively).

A coupled model of carbon-water exchange of the Amazon rain forest

E. Simon et al.

[Title Page](#)

[Abstract](#)

[Introduction](#)

[Conclusions](#)

[References](#)

[Tables](#)

[Figures](#)

◀

▶

◀

▶

[Back](#)

[Close](#)

[Full Screen / Esc](#)

[Print Version](#)

[Interactive Discussion](#)

– The sensitivity of predicted canopy net energy and CO₂ fluxes to the selection of these parameters highlights the demand on ecophysiological measurements and their use and application in detailed models of surface-atmosphere exchange, as presented.

5 – In contrast to the large sensitivity to leaf scale parameters (5–34%), the uncertainty of predicted canopy fluxes resulting from the uncertainty of canopy structure, i.e. total LAI, is low (1–12%).

10 – The derived distribution function for canopy structure agrees well with available observations. Site specific modifications can be achieved by changing the function scaling and shape parameters.

15 – An optimum number of 8 canopy layers ($\Delta z=5$ m) is derived for model application. The predicted canopy albedo is relatively insensitive to total leaf area, but strongly dependent on leaf optical parameters. Best agreement with observations is obtained when recommended values for reflectance and transmittance are reduced by 25–40%.

20 – Also demonstrated by comparison with observations is the high accuracy of predicted PAR fractions of incoming radiation. Due to underestimation of atmospheric emissivity under high emissivity conditions, the simulated incoming long wave radiation is systematically underestimated (1–5%), equivalent to a maximum of 25 W m⁻² at noon time.

25 – Mean incident light observed at different sites show a similar extinction in different canopy layers when attenuation is related to vertical canopy position. A good correspondence is obtained between PAR measurements and predicted mean PAR absorbed by sunlit and shaded leaves using a canopy radiation model.

– Although the scaling of canopy biochemistry remains uncertain, available field data supports the light acclimation hypothesis for Amazon rain forest. While ir-

A coupled model of carbon-water exchange of the Amazon rain forest

E. Simon et al.

[Title Page](#)

[Abstract](#)

[Introduction](#)

[Conclusions](#)

[References](#)

[Tables](#)

[Figures](#)

◀

▶

◀

▶

[Back](#)

[Close](#)

[Full Screen / Esc](#)

[Print Version](#)

[Interactive Discussion](#)

radiance decreases exponentially with accumulated leaf area, photosynthetic capacity was found to decrease nearly linearly.

BGD

2, 333–397, 2005

5. Spatial integration

For an arbitrary tracer, the net flux at the canopy top (F) is given by the sum of integrated sources and sinks of all layers ($S_i \Delta z_i$) according to

$$F = \sum_i^m S_i \Delta z_i. \quad (7)$$

Each layer has a leaf area $\Delta \Lambda_i$ which is used to scale up leaf exchange (F_{leaf}) by

$$S_i \Delta z_i = \Delta \Lambda_i F_{leaf}(z_i). \quad (8)$$

The exchange of sunlit and shaded leaves is treated separately. Therefore, Λ_i is divided into a sunlit and shaded part, determined by the fraction of sunlit leaves in each layer. For each time step, the ambient air temperature and concentrations of H_2O and CO_2 in each canopy layer are initialized with their values given above the canopy (Table 3). After calculating the absorbed short-wave radiation, the energy balance is solved numerically, separately for sunlit and shaded leaves. After applying Eq. (8), C_a is changed by

$$\Delta C_a(z_j) = \sum_i^m d(i, j) S_i \Delta z_i \quad (9)$$

where $d(i, j)$ represents the coefficients of the dispersion matrix connecting the temperature and concentration change $\Delta C_a(z_j)$ with S_i . Equations (8)–(9) are repeated until the summed absolute temperature change in all layers is less than 0.01 K.

A coupled model of carbon-water exchange of the Amazon rain forest

E. Simon et al.

[Title Page](#)

[Abstract](#)

[Introduction](#)

[Conclusions](#)

[References](#)

[Tables](#)

[Figures](#)

[◀](#)

[▶](#)

[◀](#)

[▶](#)

[Back](#)

[Close](#)

[Full Screen / Esc](#)

[Print Version](#)

[Interactive Discussion](#)

EGU

6. Leaf surface exchange

BGD

2, 333–397, 2005

A detailed description of the coupled equations of leaf surface exchange is given by [Leuning et al. \(1995\)](#). In general, net radiation at the leaf surface (Q_n) can be either expressed in terms of a radiation budget or a budget of mass fluxes. The radiation budget gives

$$Q_n = Q_{SW} \downarrow - Q_{SW} \uparrow + Q_{LW} \downarrow - Q_{LW} \uparrow \quad (10)$$

where Q_{SW} and Q_{LW} are the short- and long-wave radiation, respectively. For steady-state conditions, Q_n represents the available energy that is mainly converted into latent (LE) and sensible heat (H), giving the budget of mass fluxes according to

$$Q_n = \lambda^m E + H - \lambda^C A_n \quad (11)$$

where λ^m is the molar latent heat of vaporization. $\lambda^C A_n$ represents the chemical energy of CO_2 fixation (according to [Jones, 1992](#), the energy storage into leaf tissue is usually <5% on a timescale of one hour). All terms on the right hand side of Eq. (11) can be expressed in a flux-gradient relationship

$$E = g_{tw}(D_a + s\Delta T) \quad (12)$$

$$H = g_{tH} c_p^m \Delta T \quad (13)$$

$$A_n = g_{tc} \Delta c, \quad (14)$$

where g_t are the total molar conductance for water vapor, heat, and CO_2 , denoted by subscripts w , H , and c , respectively. $(D_a + s\Delta T)$, ΔT , and Δc , are the scalar gradients of water vapor pressure, temperature, and CO_2 across the surface pathway from inside the leaf to the ambient air, respectively. s and c_p^m are the the slope relating water vapor pressure to temperature (de/dT in units of hPa K^{-1}) and the molar specific heat of dry air, respectively. For stomatal controlled transfer (CO_2 , H_2O), g_t can be decomposed to $1/g_t = 1/g_s + 1/g_b$ ([Ball, 1987](#)) where g_s and g_b are the leaf stomatal

A coupled model of carbon-water exchange of the Amazon rain forest

E. Simon et al.

[Title Page](#)

[Abstract](#)

[Introduction](#)

[Conclusions](#)

[References](#)

[Tables](#)

[Figures](#)

◀

▶

◀

▶

[Back](#)

[Close](#)

[Full Screen / Esc](#)

[Print Version](#)

[Interactive Discussion](#)

EGU

and boundary-layer conductance, respectively. For steady state conditions, Eqs. (11–13) can be combined to the Penman-Monteith equation (Monteith, 1965) as

$$\lambda^m E = \frac{Q_n + c_p^m D_a g_{tH}}{1 + \frac{\gamma_{air}}{s} [1 + (g_t H / g_{tw})]}, \quad (15)$$

where γ_{air} is the psychrometric constant (hPa K⁻¹).

Stomatal conductance for CO₂ (g_{sc}) is linked to A_n using the semi-empirical relationship of Ball et al. (1987), hereafter referred to as B87, giving

$$g_{sc} = g_{s0} + a_A A_n RH_s / c_s, \quad (16)$$

where g_{s0} is the minimum stomatal conductance, RH_s the relative humidity at the leaf surface, and a_A an empirical coefficient relating g_s to A_n . The B87 model has been

modified by replacing the dependence on RH_s by a function of water pressure deficit $f(D)$ and by including a CO₂ compensation point (Γ) to avoid $c_s \rightarrow 0$ (Leuning, 1990; Lloyd, 1991). Note that some authors also include empirically the role of water availability in the root zone (Wang and Leuning, 1998; Tuzet et al., 2003). Using the Lohammer function $f(D) = 1 + D_s / D_{s0}$ for humidity response (Lohammer et al., 1980), where D_s is the water vapor pressure deficit at the leaf surface and D_{s0} an empirical coefficient, the B87 model is rewritten into the form of Leuning et al. (1995) to

$$g_{sc} = g_{s0} + \frac{a_A A_n}{(c_s - \Gamma)(1 + \frac{D_s}{D_{s0}})} \quad (17)$$

g_s for water and other scalars can be obtained by multiplying g_{sc} with the ratio of molecular diffusivities (Ball, 1987).

The biochemical leaf model of leaf photosynthesis for C₃ plants was originally developed by Farquhar et al. (1980) and Caemmerer and Farquhar (1981). We implemented the combined approach of Leuning et al. (1995), who identify three different processes constraining A_n : (1) the biochemical demand for CO₂ inside the chloroplast,

A coupled model of carbon-water exchange of the Amazon rain forest

E. Simon et al.

[Title Page](#)

[Abstract](#)

[Introduction](#)

[Conclusions](#)

[References](#)

[Tables](#)

[Figures](#)

◀

▶

◀

▶

[Back](#)

[Close](#)

[Full Screen / Esc](#)

[Print Version](#)

[Interactive Discussion](#)

(2) the supply of CO_2 by diffusion through the stomata and the leaf boundary layer ($c_i = c_a + A_n/g_t$, Eq. 14) and (3) the stomatal response to A_n (Eq. 17) which constrains again the demand function. A general description for the demand of CO_2 is given by

$$A_n = \min\{A_V, A_J\} - R_d \quad (18)$$

5 where A_V is the gross rate of photosynthesis limited by the biochemical fixation of CO_2 and A_J the rate of photosynthesis limited by the regeneration of CO_2 acceptors. In the case of C_3 plants, A_V is limited by the CO_2 dependent activity of Ribulose bisphosphate carboxylase-oxygenase (Rubisco) v_{cmax} , which depends on CO_2 and oxygen concentration (o_i) inside the leaf and the Michaelis coefficients for carboxylation (K_c) and oxygenation (K_o) according to

$$A_V = v_{cmax} \frac{c_i - \Gamma_*}{c_i + K_c(1 + o_i/K_o)}. \quad (19)$$

10 For C_4 plants, a similar approach has been developed by Collatz et al. (1992). A_J is limited by the regeneration of Ribulose bisphosphate (RuP_2), which depends on the light driven rate of electron transport across the chloroplast membrane (J). The actual rate J is the smaller root of a hyperbolic function, determined by the maximum rate for electron transport (J_{\max}), leaf absorbed radiation (Q_{abs}), light use efficiency (α) and a parameter determining the shape of the transition of the rectangular light response curve from linear increase to saturation (θ):

$$\theta J^2 - (\alpha Q_{abs} + J_{\max})J + \alpha Q_{abs} J_{\max} = 0. \quad (20)$$

15 20 All parameter values required to solve the coupled leaf model are listed in Table 7. Leaf respiration (R_d) and the maximum rate of electron transport (J_{\max}) at a reference leaf temperature T_{s0} are calculated as a fixed proportion of v_{cmax0} . Temperature kinetics of R_d , K_c and K_o are calculated according to Harley et al. (1992) and Leuning et al. (1995), requiring appropriate values for activation (H_a) and deactivation (H_d) and, for 25 v_{cmax} and J_{\max} also for entropy (S_V, S_J). The coefficients γ_{0-2} , listed in Table 7, are

A coupled model of carbon-water exchange of the Amazon rain forest

E. Simon et al.

[Title Page](#)

[Abstract](#)

[Introduction](#)

[Conclusions](#)

[References](#)

[Tables](#)

[Figures](#)

◀

▶

◀

▶

[Back](#)

[Close](#)

[Full Screen / Esc](#)

[Print Version](#)

[Interactive Discussion](#)

required to calculate the temperature dependence of the CO₂ compensation point in the absence of day respiration.

According to Monteith (1973), the conductance at the leaf boundary-layer (g_b) can be decomposed into a forced (g_{bu}) and free convective (g_{bf}) part

$$^5 \quad g_b = g_{bu} + g_{bf}. \quad (21)$$

The single-sided forced and free convective leaf boundary layer conductance for heat (g_{buH} and g_{bHf} , respectively) are given by

$$g_{buH} = 0.003\sqrt{u/w_l} \quad (22)$$

$$g_{bHf} = 0.5D_H Gr^{1/4}/w_l \quad (23)$$

10 where u , w_l , D_H and Gr are the mean horizontal wind speed, mean leaf width, the molecular diffusivity for heat and the Grashof number, respectively. Gr is calculated from ΔT according to $Gr=1.6\times10^8|\Delta T|w_l^3$. w_l is estimated as 0.15 m from a large collection of leaves from Amazonian tree species (Ribeiro et al., 1999).

7. Radiation

15 Absorbed radiation of shaded leaves (Q_{SH}) is defined by the sum of diffusive and scattered beam radiation. The absorbed radiation of sunlit leaves (Q_{SL}) includes additionally a direct beam component leading to

$$Q_{SH}(\Lambda_z) = Q_d(\Lambda_z) + Q_{sb}(\Lambda_z) \quad (24)$$

$$Q_{SL}(\Lambda_z) = Q_b(\Lambda_z) + Q_{SH}(\Lambda_z), \quad (25)$$

20 where Λ_z is the cumulative leaf area above z . Diffusive, scattered, and direct beam components denoted by subscripts d , sb and b , respectively, are calculated according

A coupled model of carbon-water exchange of the Amazon rain forest

E. Simon et al.

[Title Page](#)

[Abstract](#)

[Introduction](#)

[Conclusions](#)

[References](#)

[Tables](#)

[Figures](#)

◀

▶

◀

▶

[Back](#)

[Close](#)

[Full Screen / Esc](#)

[Print Version](#)

[Interactive Discussion](#)

to

$$Q_d(\Lambda_z) = Q_{d0}k_d(1 - \rho_{cd}) \exp(-k_d\Lambda_z) \quad (26)$$

$$Q_{sb}(\Lambda_z) = Q_{b0}k_b(1 - \rho_{cb}) \exp(-k_b\Lambda_z) - Q_b(\Lambda_z) \quad (27)$$

$$Q_b(\Lambda_z) = Q_{b0}k_b^B(1 - \sigma_l) \exp(-k_b^B\Lambda_z), \quad (28)$$

5 where σ_l , ρ_c , and k are the scattering (reflection plus transmission), canopy reflection, and extinction coefficients, respectively. k^B is the extinction coefficient for black leaves (with no reflection or transmission). The scattered direct beam radiation is obtained by subtracting Q_b from the total absorbed beam radiation (direct + scattered). The fraction of sunlit leaves (f_{SL}) is calculated as $f_{SL}(\Lambda_z) = \exp(-k_b\Lambda_z)$

10 The net long-wave radiation of a body is generally given by

$$Q_{LW} = Q_{LW} \downarrow - Q_{LW} \uparrow = \epsilon_a \sigma_B T_a^4 - \epsilon_s \sigma_B T_s^4, \quad (29)$$

where ϵ_s , ϵ_a and T_s , T_a represent the emissivity and temperature of the body and ambient air and \downarrow and \uparrow denote the incoming and outgoing parts of Q_{LW} , respectively. σ_B is the Stefan-Boltzmann constant. ϵ_s has different values for soil and leaf surfaces given as $\epsilon_l = 0.96$ and $\epsilon_{soil} = 0.94$, respectively, (Wang and Leuning, 1998).

15 Incoming long-wave radiation ($Q_{LW\downarrow}$) is calculated analogously to diffusive radiation according to

$$Q_{LW\downarrow}(\Lambda_z) = \epsilon_{a0} \sigma_B T_{ref}^4 k_d^B \exp(-k_d^B \Lambda_z). \quad (30)$$

20 The outgoing long wave radiation given as $Q_{LW\uparrow}(\Lambda_z) = \epsilon_s \sigma_B T_s(\Lambda_z)^4$ can not be solved directly, since T_s is part of the leaf energy balance. Instead, the isothermal outgoing long wave radiation ($Q_{LW\uparrow}^*$), equivalent to the long wave radiation that would be lost, if the surface were at ambient temperature (Jones, 1992) is calculated by replacing T_{ref} and ϵ_{a0} in Eq. (30) with $T_a(\Lambda_z)$ and ϵ_s , respectively. The isothermal net radiation (Q_n^*) is then given by

$$Q_n^* = Q_{SW\downarrow} - Q_{SW\uparrow} + Q_{LW\downarrow} - Q_{LW\uparrow}^*. \quad (31)$$

A coupled model of carbon-water exchange of the Amazon rain forest

E. Simon et al.

[Title Page](#)

[Abstract](#)

[Introduction](#)

[Conclusions](#)

[References](#)

[Tables](#)

[Figures](#)

[◀](#)

[▶](#)

[◀](#)

[▶](#)

[Back](#)

[Close](#)

[Full Screen / Esc](#)

[Print Version](#)

[Interactive Discussion](#)

Combining Eqs. (31) and (10) leads to

$$Q_n^* = Q_n + \sigma_B \epsilon_s (T_s^4 - T_a^4). \quad (32)$$

The substitution $T_s = T_a + \Delta T$ followed by multiplication cancels T_a^4 out. All terms including ΔT with second or higher power can be neglected because $\Delta T \ll T_a$ and it remains

$$Q_n \simeq Q_n^* - \sigma_B \epsilon \Lambda 4T_a^3 \Delta T \quad (33)$$

where $g_{rad} = \epsilon \sigma_B 4T_a^3 / c_p^m$ is defined as the radiative conductance.

8. Parameterization of soil surface exchange

Soil evaporation is calculated by solving the Penman-Monteith equation for a bulk soil surface layer from -0.05 to 1 m height. The solution, described in more detail in Garrat (1992), requires the soil relative humidity (RH_{soil}) and the bulk soil surface conductance (g_{soil}) as input parameters. RH_{soil} is related to the soil matrix potential (ψ_{soil}) according to

$$RH_{soil} = \exp \left(\frac{-g\psi_{soil}}{RT_{soil}} \right), \quad (34)$$

whereas g and R are the gravity and the universal gas constant, respectively. ψ_{soil} is calculated from the volumetric soil water content (η_w) according to

$$\psi_{soil} = \psi_{soil}^* (\eta_w / \eta_w^*)^{-a_\psi} \quad (35)$$

with η_w^* , ψ_{soil}^* , and a_ψ being the total soil pore space, ψ_{soil} at saturation and an empirical coefficient, respectively. For a sandy loam, which is the dominant soil type at the Jaru site, Garrat (1992) proposes a maximum matrix potential of $\psi_{soil}^* = -0.218$, a

[Title Page](#)

[Abstract](#)

[Introduction](#)

[Conclusions](#)

[References](#)

[Tables](#)

[Figures](#)

◀

▶

◀

▶

[Back](#)

[Close](#)

[Full Screen / Esc](#)

[Print Version](#)

[Interactive Discussion](#)

coefficient value of $a_w=4.9$, and a maximum water filled pore space of $\eta_w^* \approx 0.5$ which is in agreement with the value given by Gut et al. (2002b) for the Jaru site.

For soil respiration (F_{csoil}), the simple Arrhenius curve

$$F_{csoil} = F_{csoil0} \exp [H_{asoil}/RT_{soil0} (1 - T_{soil0}/T_{soil})] \quad (36)$$

is applied, where F_{csoil0} is the soil respiration at a reference temperature T_{soil0} and H_{asoil} the activation energy (Tuzet et al., 2003).

List of symbols

α quantum yield of whole-chain electron transport (-)

$\epsilon_{a0,s}$ long-wave emissivity with subscripts $a0$ and s denoting the atmosphere and surface (leaves and soil), respectively (-)

η_w, η_w^* water filled pore space, total soil pore space (-)

Γ CO_2 compensation point ($\mu\text{mol mol}^{-1}$)

Γ_* CO_2 compensation point in the absence of day respiration ($\mu\text{mol mol}^{-1}$)

$\gamma_{0,1,2}$ empirical constants required to calculate Γ_* (-)

γ_{air} psychometric constant (hPa K^{-1})

λ^m latent heat of vaporization for water (J mol^{-1})

λ^c chemical energy stored by CO_2 fixation ($\text{J } \mu\text{mol}^{-1}$)

$\Lambda_{0,z,hc}$ accumulated leaf area with subscripts $0, z, hc$ denoting total LAI, at height z and (zero) at the canopy top ($\text{m}^2 \text{ m}^{-2}$)

BGD

2, 333–397, 2005

A coupled model of carbon-water exchange of the Amazon rain forest

E. Simon et al.

[Title Page](#)

[Abstract](#)

[Introduction](#)

[Conclusions](#)

[References](#)

[Tables](#)

[Figures](#)

[◀](#)

[▶](#)

[◀](#)

[▶](#)

[Back](#)

[Close](#)

[Full Screen / Esc](#)

[Print Version](#)

[Interactive Discussion](#)

EGU

ψ_{soil} soil matrix potential with superscript * denoting maximum ψ_{soil} (-)

BGD

ρ_{cx} canopy reflection coefficient with subscripts $x = d, b$ and N, V denoting diffusive or beam, and visible or near-infrared radiation, respectively (-)

2, 333–397, 2005

ρ_h canopy reflection coefficient for horizontal leaves (-)

5 σ_B Stefan-Boltzmann constant (5.67051×10^{-8}) ($\text{W m}^{-2} \text{K}^{-4}$)

σ_{lx} scattering coefficient with subscripts $x = d, b$ and N, V denoting diffusive or beam, and visible or near-infrared radiation, respectively (-)

θ shape coefficient of the hyperbolic light response function for photosynthesis (-)

A_J gross rate of photosynthesis limited by RuP₂ regeneration ($\mu\text{mol m}^{-2} \text{s}^{-1}$)

10 A_n net assimilation rate ($\mu\text{mol m}^{-2} \text{s}^{-1}$)

A_v gross rate of photosynthesis limited by Rubisco activity ($\mu\text{mol m}^{-2} \text{s}^{-1}$)

a_A empirical parameter relating stomatal conductance to assimilation (-)

$a_{i1,2}$ coefficients in Eq. (1) with $i = T, B$ for top and bottom canopy layer, respectively (-)

15 C_x scalar concentration with subscripts s, a, ref denoting the leaf surface, ambient air, and reference height level, respectively

c_N leaf nitrogen concentration (mmol m^{-2})

c_p^m specific heat of air ($\text{J mol}^{-1} \text{K}^{-1}$)

20 c_x CO₂ concentration with subscripts $soil, i, s, a, ref$ denoting the soil, intercellular, leaf surface, ambient air, and reference height level, respectively ($\mu\text{mol mol}^{-1}$)

A coupled model of carbon-water exchange of the Amazon rain forest

E. Simon et al.

[Title Page](#)

[Abstract](#)

[Introduction](#)

[Conclusions](#)

[References](#)

[Tables](#)

[Figures](#)

◀

▶

◀

▶

[Back](#)

[Close](#)

[Full Screen / Esc](#)

[Print Version](#)

[Interactive Discussion](#)

EGU

D_{s0} empirical coefficient reflecting the stomatal sensitivity to D_s (hPa)

D_x water vapor pressure deficit with subscripts *soil*, *i*, *s*, *a*, *ref* denoting the soil, intercellular, leaf surface, ambient air, and reference height level, respectively (hPa)

d_h zero length displacement height (m)

${}_5d(i, j)$ dispersion coefficient from layer *i* to layer *j* ($\text{m}^{-2} \text{ s}^{-1}$)

E leaf transpiration ($\text{mmol m}^{-2} \text{ s}^{-1}$)

F trace gas flux expressed on ground area

F_{csoil} soil respiration with subscript 0 denoting F_{csoil} at T_{soil0} ($\text{μmol m}^{-2} \text{ s}^{-1}$)

F_{leaf} trace gas flux expressed on leaf area

${}^{10}f_{SL,SH}$ sunlit (*SL*) or shaded (*SH*) leaf fraction (-)

$f_{d,b}$ diffusive (*d*) or direct beam (*b*) fraction of radiation (-)

G soil heat flux (W m^{-2})

Gr Grashof number (-)

15

g_b leaf boundary layer conductance with subscripts *H*, *w*, *c* denoting heat, water, and CO_2 , and *u*, *f* denoting the convective and forced part of g_b , respectively ($\text{mol m}^{-2} \text{ s}^{-1}$)

g_{rad} radiative conductance ($\text{mol m}^{-2} \text{ s}^{-1}$)

g_s stomatal conductance with subscripts *w* and *c* denoting water and CO_2 ($\text{mol m}^{-2} \text{ s}^{-1}$)

BGD

2, 333–397, 2005

A coupled model of carbon-water exchange of the Amazon rain forest

E. Simon et al.

[Title Page](#)

[Abstract](#)

[Introduction](#)

[Conclusions](#)

[References](#)

[Tables](#)

[Figures](#)

[◀](#)

[▶](#)

[◀](#)

[▶](#)

[Back](#)

[Close](#)

[Full Screen / Esc](#)

[Print Version](#)

[Interactive Discussion](#)

g_t total conductance with subscripts H , w , c denoting heat, water, and CO_2 ($\text{mol m}^{-2} \text{s}^{-1}$)

$gRad$ incoming global radiation with subscript 0 denoting potential global radiation (W m^{-2})

5 H sensible heat flux (W m^{-2})

H_x energy with subscripts d and v and Ko, Kc, Rd, V, J , and *soil* denoting the activation and deactivation of $K_c, K_o, R_d, V_{cmax}, J_{max}$, and F_{csoil} , respectively (J mol^{-1})

h_c mean canopy height (m)

10 I_x the incomplete beta function

J electron transport rate ($\mu\text{mol m}^{-2} \text{s}^{-1}$)

J_{max} potential rate of electron transport with subscript 0 denoting J_{max} at T_{s0} ($\mu\text{mol m}^{-2} \text{s}^{-1}$)

15 $K_{c,o}$ Michaelis coefficient with subscript c and o denoting for carboxylation and oxygenation, respectively ($\mu\text{mol m}^{-2} \text{s}^{-1}$)

k_N extinction coefficient for c_N (-)

$k_{d,b}^{(B)}$ extinction coefficient for diffusive (d) or beam (b) radiation with superscript B denoting black leaves (-)

k_u extinction coefficient for u (-)

20 L_s canopy length scale (m)

LE canopy latent heat flux (W m^{-2})

A coupled model of carbon-water exchange of the Amazon rain forest

E. Simon et al.

[Title Page](#)

[Abstract](#)

[Introduction](#)

[Conclusions](#)

[References](#)

[Tables](#)

[Figures](#)

◀

▶

◀

▶

[Back](#)

[Close](#)

[Full Screen / Esc](#)

[Print Version](#)

[Interactive Discussion](#)

o_i intercellular oxygen concentration (mmol mol $^{-1}$)

P_0 air pressure at the reference height (hPa)

Q_{10} change rate of a biological process for a temperature increase of 10°C (-)

Q_{LW} long wave radiation with \downarrow and \uparrow indicating incoming and outgoing direction, respectively (W m $^{-2}$)

$Q_{N0,V0}$ incoming visible ($V0$) or near-infrared ($N0$) radiation (W m $^{-2}$)

Q_{PAR} photosynthetic active radiation ($\mu\text{mol m}^{-2} \text{ s}^{-1}$)

$Q_{SH,SL}$ radiation absorbed by sunlit (SL) or shaded (SH) leaves (W m $^{-2}$)

Q_{SW} short-wave radiation (W m $^{-2}$)

$Q_{d,b,sb}$ diffusive (d), direct beam (b) or scattered (sb) beam radiation (W m $^{-2}$)

Q_n net radiation (W m $^{-2}$)

Q_n^* isothermal net radiation assuming $T_s = T_a$ (W m $^{-2}$)

R universal gas constant (8.3145 J mol $^{-1}$ K $^{-1}$)

R_d day respiration ($\mu\text{mol m}^{-2} \text{ s}^{-1}$)

RH_x relative humidity with subscripts *soil*, *i*, *s*, *a*, *ref* denoting the soil, intercellular, leaf surface, ambient air, and reference height level, respectively (-)

$S_{v,d}$ entropy for activation (v) and deactivation (d) (J mol $^{-1}$)

S_i source/sink strength of layer i

A coupled model of carbon-water exchange of the Amazon rain forest

E. Simon et al.

[Title Page](#)

[Abstract](#)

[Introduction](#)

[Conclusions](#)

[References](#)

[Tables](#)

[Figures](#)

◀

▶

◀

▶

[Back](#)

[Close](#)

[Full Screen / Esc](#)

[Print Version](#)

[Interactive Discussion](#)

A coupled model of carbon-water exchange of the Amazon rain forest

E. Simon et al.

s slope of the curve relating saturation water vapor pressure to temperature (hPa K⁻¹)

T_x temperature with subscripts *soil*, *s*, *a*, *ref* denoting the soil, leaf surface, ambient air, and reference height level, respectively (K)

⁵ *T_{x0}* reference temperature (K)

t_d time of the year (d)

t_h local solar time (h)

u horizontal wind speed with subscript *ref* denoting the reference height (m s⁻¹)

¹⁰ *V_{cmax}* maximum catalytic activity of Rubisco, ($\mu\text{mol m}^{-2} \text{s}^{-1}$, subscripts 0 and *hc* denote *V_{max}* at *T_{s0}* and at the canopy top, respectively)

w_i weight coefficients in Eq. (1) with *i* = *T* and *i* = *B* for top and bottom canopy maximum of leaf area density (-)

w_l mean leaf width (m)

z height above ground (m)

¹⁵ *z₀* roughness length (m)

z_{ref} reference height above *h_c* (m)

z_i mean layer height (m)

z_i^{}* upper boundary of a single leaf area distribution (m)

Acknowledgements. We would like to thank many people for providing high quality field data from Amazonia, especially U. Rummel, U. Kuhn, S. Rottenberger, C. Ammann, A. Gut, G. Kirkman (MPIC), B. Kruijt and J. Elbers (Alterra-Institute), J. Lloyd (University of Leeds) and representatively for the pre-LBA studies the UK Institute of Hydrology for making the ABRACOS data sets available. The research is supported by the Max Planck Society and the European Union (EUSTACH-LBA; ENV4-CT97-0566).

5 Andreae, M. O., Artaxo, P., Brando, C., Carswell, F. E., Ciccioli, P., da Costa, A. L., Culf, A. D., Esteves, J. L., Gash, J. H. C., Grace, J., Kabat, P., Lelieveld, J., Malhi, Y., Manzi, A. O., Meixner, F. X., Nobre, A. D., Nobre, C., Ruivo, M., Silva-Dias, M. A., Stefani, P., Valentini, R., von Jouanne, J., and Waterloo, M. J.: Biogeochemical cycling of carbon, water, energy, trace gases, and aerosols in Amazonia: The LBA-EUSTACH experiments, *J. Geophys. Res.*, 107, 33.1–33.25, 2002. [336](#), [337](#), [338](#), [339](#), [345](#), [377](#), [378](#)

10 Araujo, A., Nobre, A., Kruijt, B., Elbers, J., Dallarosa, R., Stefani, P., von Randow, C., Manzi, A., Culf, A., Gash, J., Valentini, R., and Kabat, P.: Comparative measurements of carbon dioxide fluxes from two nearby towers in a central Amazonian rainforest: The Manaus LBA site, *J. Geophys. Res.*, 107, 58.1–58.20, 2002. [378](#)

15 Baldocchi, D.: A Lagrangian random-walk model for simulating water vapour, CO_2 and sensible heat flux densities and scalar profiles over and within a soybean canopy, *Bound.-Layer Meteorol.*, 61, 113–144, 1992. [335](#)

20 Baldocchi, D. and Bowling, D. R.: Modelling the discrimination of $^{13}\text{CO}_2$ above and within a temperate broad-leaved forest canopy on hourly to seasonal timescales, *Plant, Cell Env.*, 26, 231–244, 2003. [336](#)

25 Baldocchi, D. and Harley, P.: Scaling carbon dioxide and water vapour exchange from leaf to canopy in a deciduous forest: Model testing and application, *Plant, Cell Env.*, 18, 1157–1173, 1995. [336](#)

30 Baldocchi, D. and Meyers, T.: On using eco-physiological, micrometeorological and biogeochemical theory to evaluate carbon dioxide, water vapor and trace gas fluxes over vegetation – a perspective, *Agric. For. Meteorol.*, 90, 1–25, 1998. [335](#), [336](#), [337](#)

Ball, J.: Calculations related to gas exchange, in *Stomatal Function*, edited by: Zeiger, E., Farquhar, G., and Cowan, I., Stanford University Press, Stanford, California, 445–476, 1987. [350](#), [357](#), [358](#)

35 Ball, J., Woodrow, I., and Berry, J.: A model predicting stomatal conductance and its contribution to the control of photosynthesis under different environmental conditions, in: *Progress in Photosynthesis Research*, edited by: Biggins, I., Martinus Nijhoff, Netherlands, 221–224,

A coupled model of carbon-water exchange of the Amazon rain forest

E. Simon et al.

[Title Page](#)

[Abstract](#)

[Introduction](#)

[Conclusions](#)

[References](#)

[Tables](#)

[Figures](#)

◀

▶

◀

▶

[Back](#)

[Close](#)

[Full Screen / Esc](#)

[Print Version](#)

[Interactive Discussion](#)

1987. 336, 341, 351, 358, 396

Brutsaert, W.: On a derivable formula for long-wave radiation for clear skies, *Water Resources Research*, 11, 742–744, 1975. 339, 343

Caemmerer, S. v. and Farquhar, G. D.: Some relationships between the biochemistry of photo-synthesis and the gas exchange of leaves, *Planta*, 153, 376–387, 1981. 336, 358

5 Carswell, F., Meir, P., Wandell, E., Bonates, L., Krujt, B., Barbosa, E., Nobre, A., Grace, J., and Jarvis, P.: Photoynthetic capacity in a central Amazonian rain forest, *Tree Physiol.*, 20, 179–186, 2000. 338, 339, 348, 349, 350, 378, 392

10 Collatz, G., Ball, J., Grivet, C., and Berry, J.: Phyisiological and environmental regulation of stomatal conductance, photosynthesis and transpiration: A model that includes a laminar boundary layer, *Agric. For. Meteorol.*, 54, 107–136, 1991. 336

Collatz, G., Ribbas-Carbo, M., and Berry, J.: Coupled photosynthesis-stomatal conductance model for leaves of C4 plants, *Aust. J. Plant Physiol.*, 54, 107–136, 1992. 336, 359

15 Culf, A., Fisch, G., and Hodnett, M.: The albedo of Amazonian forest ranch land, *J. Climate*, 8, 1543–1554, 1995. 339, 347, 378, 390

Culf, A., Esteves, J. L., Filho, M. O., and Rocha, H. d.: Radiation, temperature and humidity over forest and pasture in Amazonia, in *Amazonian Deforestation and Climate*, edited by: Gash, J., Nobre, C., Roberts, J., and Victoria, R., John Wiley and Sons, Chichester, 177–191, 1996. 339, 347, 378, 390

20 Deardorff, J.: Efficient prediction of ground surface temperature and moisture with inclusion of a layer of vegetation, *J. Geophys. Res.*, 83, 1889–1903, 1978. 335

Dickinson, R. E., Henderson-Sellers, A., and Kennedy, P. J.: Biosphere-Atmosphere Transfer Scheme (BATS) version 1e as coupled to the NCAR community climate model, NCAR Technical Note 387, NCAR, 1993. 335

25 Eschenbach, C. and Kappen, L.: Leaf area index determination in an alder forest – a comparison of three methods, *Journal of Experimental Botany*, 47, 1457–1462, 1996. 339

Evans, J.: Photosynthesis and nitrogen relationships in leaves of C3 plants, *Oecologia*, 78, 9–19, 1989. 341

30 Falge, E., Baldocchi, D., Tenhunen, J., Aubinet, M., Bakwin, P., Berbigier, P., Bernhofer, C., Burba, G., Clement, R., Davis, K. J., Elbers, J. A., Goldstein, A. H., Grelle, A., Granier, A., Guomundsson, J., Hollinger, D., Kowalski, A. S., Katul, G., Law, B. E., Malhi, Y., Meyers, T., Monson, R. K., Munger, J. W., Oechel, W., Paw U, K. T., and et al.: Seasonality of ecosystem respiration and gross primary production as derived from FLUXNET measurements, *Agric.*

BGD

2, 333–397, 2005

A coupled model of carbon-water exchange of the Amazon rain forest

E. Simon et al.

[Title Page](#)

[Abstract](#)

[Introduction](#)

[Conclusions](#)

[References](#)

[Tables](#)

[Figures](#)

[◀](#)

[▶](#)

[◀](#)

[▶](#)

[Back](#)

[Close](#)

[Full Screen / Esc](#)

[Print Version](#)

[Interactive Discussion](#)

EGU

For. Meteorol., 113, 53–74, 2002. [336](#)

Farquhar, G. D., Caemmerer, S. v., and Berry, J.: A biochemical model of photosynthetic CO₂ assimilation in leaves of C₃-species, *Planta*, 149, 78–90, 1980. [336](#), [358](#)

Field, C.: Allocating leaf nitrogen for the maximization of carbon gain: leaf age as a control on the allocation program, *Oecologia*, 56, 341–347, 1983. [336](#), [341](#), [342](#)

Field, C. and Mooney, H.: The photosynthesis-nitrogen relationship in wild plants, in *On the Economy of Plant Form and Function*, edited by: Givnish, T., Cambridge University Press, 25–55, 1986. [341](#)

Ganzeveld, L. and Lelieveld, J.: Dry deposition parameterization in a chemistry general circulation model and its influence on the distribution of reactive trace gases, *J. Geophys. Res.*, 100, 20 999–21 012, 1995. [335](#)

Garrat, J.: *The Atmospheric Boundary Layer*, Cambridge Atmospheric and Space Science Series, Cambridge University Press, Cambridge, 1992. [341](#), [362](#), [384](#)

Gash, J., Nobre, C., Roberts, J., and Victoria, R.: An overview of ABRACOS, in *Amazonian Deforestation and Climate*, edited by: Gash, J., Nobre, C., Roberts, J., and Victoria, R., John Wiley and Sons, Chichester, 1–14, 1996. [336](#), [338](#)

Goudriaan, J. and van Laar, H.: *Modelling Crop Growth Processes*, Kluwer, Amsterdam, 1994. [341](#), [347](#)

Grace, J., Lloyd, J., McIntyre, J., Miranda, A., Meir, P., Miranda, H., Moncrieff, J., Massheder, J., Wright, I., and Gash, J.: Fluxes of carbon dioxide and water vapour over an undisturbed tropical rain forest in south-west Amazonia, *Glob. Clim. Change*, 1, 1–12, 1995. [336](#), [338](#)

Gu, L. H. and Baldocchi, D.: Fluxnet 2000 synthesis – foreword, *Agric. For. Meteorol.*, 113, 1–2, 2002. [336](#)

Gut, A., Scheibe, M., Rottenberger, S., Rummel, U., Welling, M., Ammann, C., Kirkman, G., Kuhn, U., Meixner, F., Kesselmeier, J., Lehmann, B., Schmidt, J., Mller, E., and Piedade, M.: Exchange of NO₂ and O₃ at soil and leaf surfaces in an Amazonian rain forest, *J. Geophys. Res.*, 107, 27.1–27.15, 2002a. [340](#), [349](#), [378](#)

Gut, A., van Dijk, S., Scheibe, M., Rummel, U., Welling, M., Ammann, C., Meixner, F., Kirkman, G., Andreae, M., and Lehmann, B.: NO emission from an Amazonian rain forest soil: Continuous measurements of NO flux and soil concentration, *J. Geophys. Res.*, 102, 24.1–24.10, 2002b. [363](#)

Halldin, S., Bergstrom, H., Gustafsson, D., Dahlgren, L., Hjelm, P., Lundin, L. C., Mellander, P. E., Nord, T., Jansson, P. E., Seibert, J., Stahli, M., Kishne, A. S., and Smedman, A. S.: 2, 333–397, 2005

BGD

2, 333–397, 2005

A coupled model of carbon-water exchange of the Amazon rain forest

E. Simon et al.

[Title Page](#)

[Abstract](#)

[Introduction](#)

[Conclusions](#)

[References](#)

[Tables](#)

[Figures](#)

◀

▶

◀

▶

[Back](#)

[Close](#)

[Full Screen / Esc](#)

[Print Version](#)

[Interactive Discussion](#)

EGU

A coupled model of carbon-water exchange of the Amazon rain forest

E. Simon et al.

[Title Page](#)

[Abstract](#)

[Introduction](#)

[Conclusions](#)

[References](#)

[Tables](#)

[Figures](#)

[◀](#)

[▶](#)

[◀](#)

[▶](#)

[Back](#)

[Close](#)

[Full Screen / Esc](#)

[Print Version](#)

[Interactive Discussion](#)

Continuous long-term measurements of soil-plant-atmosphere variables at an agricultural site, *Agric. For. Meteorol.*, 98–9, 75–102, 1999. [336](#)

Harley, P., Thomas, R., Reynolds, J., and Strain, B.: Modelling photosynthesis of cotton grown in elevated CO₂, *Plant, Cell Env.*, 15, 1992. [350](#), [351](#), [359](#), [383](#)

5 Hirose, T. and Bazzaz, F. A.: Trade-off between light- and nitrogen-use efficiency in canopy photosynthesis, *Ann. Bot.*, 82, 195–202, 1998. [342](#)

Hirose, T. and Werger, M.: Nitrogen use efficiency in instantaneous and daily photosynthesis of leaves in the canopy of a *Solidago altissima* stand, *Physiologia Plantarum*, 70, 215–222, 1987. [348](#)

10 Hirose, T., Werger, M., Pons, T., and Rheeinen, J. v.: Canopy structure and leaf nitrogen distribution in a stand of *Lysimachia vulgaris* L. as influenced by stand density, *Oecologia*, 77, 1988. [336](#), [342](#)

Jarvis, P.: Scaling physiological processes, in *Scaling Physiological Processes Leaf to Globe*, edited by Ehleringer, J. R. and Field, C. B., Academic Press, San Diego – London, 115–126, 1993. [335](#), [341](#)

15 Jarvis, P. G.: The interpretation of variations in leaf water potential and stomatal conductance found in canopies in the field, *Philosophical Transactions of the Royal Society*, 273, 593–610, 1976. [351](#)

Jones, H.: *Plants and Microclimate: A Quantitative Approach to Plant Physiology*, Cambridge University Press, Cambridge, 1992. [343](#), [344](#), [347](#), [357](#), [361](#)

20 Kaimal, J. and Finnigan, J.: *Atmospheric Boundary Layer Flows*, Oxford University Press, New York, 1994. [343](#)

Katul, G., Leuning, R., and Oren, R.: Relationship between plant hydraulic and biochemical properties derived from a steady-state coupled water and carbon transport model, *Plant Cell and Environment*, 26, 339–350, 2003. [336](#)

25 Katul, G. G. and Albertson, J. D.: Modeling CO₂ sources, sinks, and fluxes within a forest canopy, *J. Geophys. Res.*, 104, 6081–6091, 1999. [336](#)

Klinge, H.: Struktur und Artenreichtum des zentralamazonischen Regenwaldes, *Amazoniana*, 4, 283–292, 1973. [378](#)

30 Klinge, H., Rodrigues, W., Brunig, E., and Fittkau, E.: Biomass and structure in a central Amazonian rain forest, in *Tropical Ecological Systems. Trends in Terrestrial and Aquatic Research*, edited by: Golley, F. and Medina, E., Springer, Berlin, 115–122, 1975. [345](#), [378](#)

Kruijt, B., Malhi, Y., Lloyd, J., Nobre, A., Miranda, A., Pereira, M., Culf, A., and Grace, J.: Turbu-

lence statistics above and within two Amazon rain forest canopies, *Bound.-Layer Meteorol.*, 94, 297–331, 2000. [338, 345](#)

BGD

2, 333–397, 2005

5 Kuhn, U., Rottenberger, S., Biesenthal, T., Ammann, C., Wolf, A., Schebeske, G., Ciccioli, P., Branaleoni, E., Frattoni, M., Tavares, T., and Kesselmeier, J.: Isoprene and monoterpene emissions of Amazonian tree species during the wet season: Direct and indirect investigations on controlling environmental functions, *J. Geophys. Res.*, 107, 38.1–38.13, 2002. [340, 378, 394](#)

10 Kuhn, U., Rottenberger, S., Biesenthal, T., Wolf, A., Schebeske, G., Ciccioli, P., Branaleoni, E., Frattoni, M., Tavares, T., and Kesselmeier, J.: Seasonal differences in isoprene and light-dependent monoterpene emission by Amazonian tree species, *Global Change Biol.*, 10, 663–682, 2004. [340, 378, 394](#)

15 Lai, C. T., Katul, G., Ellsworth, D., and Oren, R.: Modelling vegetation-atmosphere CO_2 exchange by a coupled Eulerian-Lagrangian approach, *Bound.-Layer Meteorol.*, 95, 91–122, 2000a. [336](#)

20 Lai, C. T., Katul, G., Oren, R., Ellsworth, D., and Schfer, K.: Modelling CO_2 and water vapor turbulent flux distributions within a forest canopy, *J. Geophys. Res.*, 105, 26 333–26 351, 2000b. [336](#)

25 Laurance, W. F.: Mega-development trends in the Amazon: Implications for global change, *Env. Monit. Assessment*, 61, 113–122, 2000. [336](#)

30 Leuning, R.: Modelling stomatal behaviour and photosynthesis of *Eucalyptus grandis*, *Aust. J. Plant Physiol.*, 17, 159–175, 1990. [336, 358](#)

Leuning, R.: A critical appraisal of a combined stomatal-photosynthesis model for C_3 plants, *Plant, Cell Env.*, 18, 339–357, 1995. [336, 340, 342, 350, 351, 396](#)

35 Leuning, R., Kelliher, F. M., de Pury, D. G. G., and Schulze, E. D.: Leaf nitrogen, photosynthesis, conductance and transpiration: scaling from leaves to canopies, *Plant, Cell Env.*, 18, 1183–1200, 1995. [335, 336, 337, 341, 342, 348, 351, 357, 358, 359, 381, 383](#)

40 Lloyd: Modelling stomatal responses to environment in *Macadamia integrifolia*, *Aust. J. Plant Physiol.*, 18, 649–660, 1991. [336, 358](#)

45 Lloyd, J., Grace, J., Miranda, A. C., Meir, P., Wong, S. C., Miranda, B. S., Wright, I. R., Gash, J. H. C., and McIntyre, J.: A simple calibrated model of amazon rainforest productivity based on leaf biochemical properties, *Plant, Cell Env.*, 18, 1129–1145, 1995. [337, 340, 348, 349, 350, 351, 352, 378, 392](#)

50 Lohammer, T., Larsson, S., Linder, S., and Falk, S.: FAST – simulation models of gaseous

A coupled model of carbon-water exchange of the Amazon rain forest

E. Simon et al.

[Title Page](#)

[Abstract](#)

[Introduction](#)

[Conclusions](#)

[References](#)

[Tables](#)

[Figures](#)

◀

▶

◀

▶

[Back](#)

[Close](#)

[Full Screen / Esc](#)

[Print Version](#)

[Interactive Discussion](#)

EGU

exchange in Scots Pine, *Ecol. Bull.*, 32, 1980. [358](#)

McNaughton, H.: Effective stomatal boundary-layer resistances of heterogenous surfaces, *Plant, Cell Env.*, 17, 1061–1068, 1994. [342](#)

5 McWilliam, A.-L., Roberts, J., Cabral, O., Leitao, M., Costa, A. d., Maitelli, G., and Zamparini, C.: Leaf area index and above-ground biomass of terra firme rain forest and adjacent clearings in Amazonia, *Funct. Ecol.*, 7, 310–317, 1993. [345](#), [378](#), [387](#)

10 McWilliam, A.-L., Cabral, O. M. R., Gomes, B., Esteves, J. L., and Roberts, J.: Forest and pasture leaf-gas exchange in south-west Amazonia, in *Amazonian Deforestation and Climate*, edited by Gash, J., Nobre, C., Robers, J., and Victoria, R., John Wiley, Chichester, 265–285, 1996. [340](#), [351](#), [378](#), [394](#)

Meir, P., Grace, J., Miranda, A., and LLoyd, J.: Soil respiration in a rainforest in Amazonia and in cerrado in central Brazil, in *Amazonian Deforestation and Climate*, edited by ash, J., Nobre, C., Robers, J., and Victoria, R., John Wiley, Chichester, 319–329, 1996. [349](#), [393](#)

15 Meir, P., Kruijt, B., Broadmeadow, M., Barbosa, E., Kull, O., Carswell, F., Nobre, A., and Jarvis, P. G.: Acclimation of photosynthetic capacity to irradiance in tree canopies in relation to leaf nitrogen concentration and leaf mass per unit area, *Plant, Cell Env.*, 25, 343–357, 2002. [342](#), [348](#)

Meyers, T. and Paw U, K.: Testing of a higher-order closure model for modeling airflow within and above plant canopies, *Bound.-Layer Meteorol.*, 37, 297–311, 1986. [342](#)

20 Monteith, J.: Evaporation and environment, *Sym. Soc. Exp. Biol.*, 19, 206–234, 1965. [358](#)

Monteith, J.: *Principles of Environmental Physics*, Edward Arnold, London, 1973. [360](#)

Noilhan, J. and Planton, S.: A simple parameterization of land surface processes for meteorological models, *Mon. Weather Rev.*, 117, 536–549, 1989. [335](#)

25 Norman, J. and Welles, J.: Radiative transfer in an array of canopies, *Agron. J.*, 75, 481–488, 1983. [346](#)

Press, W. H.: *Numerical Recipes in C: the Art of Scientific Computing.*, vol. 1, University pressss, Cambridge, 2 edn., 1997. [342](#)

Raupach, M. R.: A Lagrangian analysis of scalar transfer in vegetation canopies, *Q. Roy. S. Meteor. Soc.*, 113, 107–120, 1987. [336](#)

30 Raupach, M. R.: A practical Lagrangian method for relating scalar concentrations to source distributions in vegetation canopies, *Quarterly Journal of the Royal Meteorological Society*, 115, 609–632, 1989. [336](#), [337](#), [340](#)

Reich, P. and Walters, M.: Photosynthesis-nitrogen relations in Amazonian tree species, *Oe-*

BGD

2, 333–397, 2005

A coupled model of carbon-water exchange of the Amazon rain forest

E. Simon et al.

[Title Page](#)

[Abstract](#)

[Introduction](#)

[Conclusions](#)

[References](#)

[Tables](#)

[Figures](#)

◀

▶

◀

▶

[Back](#)

[Close](#)

[Full Screen / Esc](#)

[Print Version](#)

[Interactive Discussion](#)

EGU

A coupled model of carbon-water exchange of the Amazon rain forest

E. Simon et al.

[Title Page](#)

[Abstract](#)

[Introduction](#)

[Conclusions](#)

[References](#)

[Tables](#)

[Figures](#)

[◀](#)

[▶](#)

[◀](#)

[▶](#)

[Back](#)

[Close](#)

[Full Screen / Esc](#)

[Print Version](#)

[Interactive Discussion](#)

cologia, 97, 73–81, 1994. [349](#)

Ribeiro, J. d. S., Hopkins, M., Vicentini, A., Sothers, C., Costa, M. d. S., Brito, J. d., Souza, M. d., Martins, L., Lohmann, L., Assuncao, P., Pereira, E. d. C., Silva, C. d., Mesquita, M., and Procopio, L.: Flora da Reserva Ducke: Guia de identificacao das plantas vasculares de uma floresta de terra-firme na Amazonia Central, INPA, Manaus, 1999. [360](#)

5 Roberts, J., Cabral Osvaldo, M. R., Fisch, G., Molion, L. C. B., Moore, C. J., and Shuttleworth, W. J.: Transpiration from an Amazonian rainforest calculated from stomatal conductance measurements, *Agric. For. Meteorol.*, 65, 175–196, 1993. [345](#), [378](#), [387](#)

10 Ross, J.: The Radiation Regime and Architecture of Plant Stands, Dr. W. Junk, Norwell, MA, 1981. [341](#), [347](#)

Rummel, U.: Turbulent exchange of ozone and nitrogen oxides from a tropical rain forest in Amazonia, Phd thesis, University Bayreuth, Germany, 2005. [339](#), [378](#)

15 Rummel, U., Ammann, C., Gut, A., Meixner, F., and Andreae, M.: Eddy covariance measurements of nitric oxide flux within an Amazonian rain forest, *J. Geophys. Res.*, 107, 17.1–17.9, 2002. [345](#)

Schulze, E.-D., Kelliher, F., Krner, C., Lloyd, J., and Leuning, R.: Relationship between maximum stomatal conductance, ecosystem surface conductance, carbon assimilation and plant nitrogen nutrition: A global ecology scaling exercise, *Annu. Rev. Ecol. Syst.*, 25, 629–660, 1994. [336](#), [341](#), [343](#), [348](#)

20 Sellers, P., Berry, J., Collatz, G., Field, C., and Hall, F.: Canopy reflectance, photosynthesis and transpiration. III: A reanalysis using improved leaf models and a new canopy integration scheme, *Remote Sens. Environ.*, 42, 187–216, 1992. [335](#)

Sellers, P., Randall, D., Collatz, G., Berry, J., Field, C., Dazlich, D., Zhang, C., Collello, G., and Bounoua, L.: A revised land surface parameterization (SIB2) for Atmospheric GCMs. Part I: Model Formulation, *J. Climate*, 9, 676–705, 1996. [335](#)

25 Sellers, P. J., Hall, F. G., Kelly, R. D., Black, A., Baldocchi, D., Berry, J., Ryan, M., Ranson, K. J., Crill, P. M., Lettenmaier, D. P., Margolis, H., Cihlar, J., Newcomer, J., Fitzjarrald, D., Jarvis, P. G., Gower, S. T., Halliwell, D., Williams, D., Goodison, B., Wickland, D. E., and Guertin, F. E.: Boreas in 1997 – experiment overview, scientific results, and future directions, *J. Geophys. Res.*, 102, 28 731–28 769, 1997. [336](#)

30 Seufert, G., Bartzis, J., Bomboi, T., Ciccioli, P., Cieslik, S., Dlugi, R., Foster, P., Hewitt, C. N., Kesselmeier, J., Kotzias, D., Lenz, R., Manes, F., Pastor, R. P., Steinbrecher, R., Torres, L., Valentini, R., and Versino, B.: An overview of the castelporziano experiments, *Atmos.*

Simon, E., Meixner, F., Rummel, U., Ganzeveld, L., Ammann, C., and Kesselmeier, J.: Coupled carbon-water exchange of the Amazon rain forest, II. Comparison of predicted and observed seasonal exchange of energy, CO₂, isoprene and ozone at a remote site in Rondonia, *Bio-geosciences Discuss.*, 2, 399–449, 2005a,

5 SRef-ID: 1810-6285/bgd/2005-2-399. 338, 352

Splitters, C.: Separating the diffusive and direct component of global radiation and its implications for modelling canopy photosynthesis, part II: Calculation of canopy photosynthesis, *Agric. For. Meteorol.*, 38, 231–242, 1986. 341

10 Tuzet, A., Perrier, A., and Leuning, R.: A coupled model of stomatal conductance, photosynthesis and transpiration, *Plant, Cell Env.*, 26, 1097–1116, 2003. 358, 363

Walters, M. and Field, C.: Photosynthetic light acclimation in two rainforest *Piper* species with different ecological amplitudes, *Oecologia*, 72, 449–456, 1987. 341

15 Wang, Y.: A comparison of three different canopy radiation models commonly used in plant modelling, *Funct. Plant Biol.*, 30, 143–152, 2003. 347

Wang, Y.-P. and Leuning, R.: A two-leaf model for canopy conductance, photosynthesis and partitioning of available energy I: Model description and comparison with a multi-layered model, *Agric. For. Meteorol.*, 91, 89–111, 1998. 340, 358, 361

20 Williams, M., Malhi, Y., Nobre, A. D., Rastetter, E. B., Grace, J., and Pereira, M. G. P.: Seasonal variation in net carbon exchange and evapotranspiration in a Brazilian rain forest: a modelling analysis, *Plant, Cell Env.*, 21, 953–968, 1998. 337

Wilson, T. B., Norman, J. M., Bland, W. L., and Kucharik, C. J.: Evaluation of the importance of Lagrangian canopy turbulence formulations in a soil-plant-atmosphere model, *Agric. For. Meteorol.*, 115, 51–69, 2003. 336

25 Wullschleger, S.: Biochemical limitations to carbon assimilation in C₃ plants - A retrospective analysis of the A/ci curves from 109 species, *Journal of Experimental Botany*, 44, 907–920, 1993. 336, 341, 348

A coupled model of carbon-water exchange of the Amazon rain forest

E. Simon et al.

[Title Page](#)

[Abstract](#)

[Introduction](#)

[Conclusions](#)

[References](#)

[Tables](#)

[Figures](#)

◀

▶

◀

▶

[Back](#)

[Close](#)

[Full Screen / Esc](#)

[Print Version](#)

[Interactive Discussion](#)

A coupled model of carbon-water exchange of the Amazon rain forest

E. Simon et al.

Table 1. Site and tower locations (see [Andreae et al., 2002](#)).

Tower	Site	Location	Elevation
RBJ-A ¹	Jaru	10°04.92' S 61°55.80' W	147 m
RBJ-B ²	Jaru	10°04.70' S 61°56.02' W	145 m
ZF2-C14 ³	Cuieiras	02°35.35' S 60°06.89' W	90 m
ZF2-K34 ¹	Cuieiras	02°35.55' S 60°12'46 W	93 m

Height: ¹53 m, ²60 m, ³40 m

[Title Page](#)

[Abstract](#)

[Introduction](#)

[Conclusions](#)

[References](#)

[Tables](#)

[Figures](#)

◀

▶

◀

▶

[Back](#)

[Close](#)

[Full Screen / Esc](#)

[Print Version](#)

[Interactive Discussion](#)

Table 2. Field data used for model parameterization and sub-model evaluation.

Section	Parameter	Site	Reference
3.1	Λ_z	Manaus	Roberts et al. (1993) ^{*,1}
		Manaus	McWilliam et al. (1993) ^{*,2}
		RBJ-A	S2005b ^{†,3}
		ZF2-C14	unpublished ^{‡,3}
		ZF2-K34	S2005b ^{‡,3}
3.2	$u(z)$	RBJ-A	Rummel (2005) [†]
3.3	albedo	RBJ-A	Culf et al. (1995, 1996) [*]
		Manaus	
3.3	$Q_{LW0\downarrow}$, Q_{PAR0}	RBJ-B	Andreae et al. (2002) [†]
		RBJ-A	Rummel (2005) [†]
	Q_{PAR0}	ZF2-K34	Araujo et al. (2002) [†]
3.3	$Q_{PAR}(\Lambda_z)$	RBJ-A	McWilliam et al. (1996) ^{*,4}
		RBJ-A	Rummel (2005) ^{†,5}
		ZF2-C14	Carswell et al. (2000) ⁴
3.4	v_{cma0hc}	ZF2-C14	Carswell et al. (2000) ⁶
		RBJ-A	Lloyd et al. (1995) ^{*,6}
3.5	F_{csoil} g_{soilH}	RBJ-A	Gut et al. (2002a) [†]
3.6	A_n A_n, g_s	RBJ-A	McWilliam et al. (1996) ^{*,6,7}
		RBJ-C	Kuhn et al. (2002, 2004) ^{†,6,8}

* Pre-LBA studies 1991–1993; [†] LBA-EUSTACH, 1999; [‡] LBA-Claire in July 2001; ¹ derived from literature data after Klinge (1973) and Klinge et al. (1975) for Reserve Ducke in the north of Manaus; ² derived by destructive sampling from adjacent clearings for a site 60 km north of Manaus; ³ optical method using LAI-2000 Plant Canopy Analyzer; ⁴ regular profiles with simultaneous measurements on different heights; ⁵ irregular profiles with subsequent measurements on different heights; ⁶ combined with leaf area (Λ_z) measurements; ⁷ porometry measurements on leaves from five tree species in different canopy layers; ⁸ 2–3 days cuvette measurements on branches from 3 tree species.

A coupled model of carbon-water exchange of the Amazon rain forest

E. Simon et al.

[Title Page](#)

[Abstract](#)

[Introduction](#)

[Conclusions](#)

[References](#)

[Tables](#)

[Figures](#)

◀

▶

◀

▶

[Back](#)

[Close](#)

[Full Screen / Esc](#)

[Print Version](#)

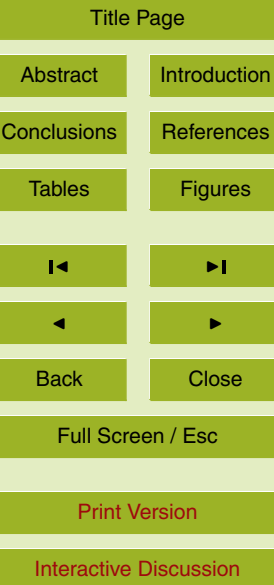
[Interactive Discussion](#)

A coupled model of carbon-water exchange of the Amazon rain forest

E. Simon et al.

Table 3. Driving variables of the canopy model (subscripts *ref* refer to the reference height above the canopy).

Parameter	Symbol	Unit
local time	t_d, t_h	[days,h]
air temperature	T_{ref}	[K]
relative humidity	RH_{ref}	[%]
barometric pressure	P_0	[hPa]
incoming global radiation	$gRad$	[W m ⁻²]
mean horizontal wind speed	u_{ref}	[m s ⁻¹]
stdev. of vertical wind speed	σ_{wref}	[m s ⁻¹]
soil temperature	T_{soil}	[K]
soil water content	η_w	[%]
bulk soil surface conduct.	g_{soilH}	[mol m ⁻² s ⁻¹]



A coupled model of carbon-water exchange of the Amazon rain forest

E. Simon et al.

Table 4. Derived parameter values for Eq. (1) (LAI $\Lambda_0 = 6$, symbols w_i , a_{i1} , a_{i2} , z_i^* represent dimensionless weights, the two parameters of the incomplete beta function and the scaling heights in units of m above ground, respectively). Numbers in brackets represent values estimated for dense ($\Lambda_0 = 6.5$ denoted as +) and open palm rich ($\Lambda_0 = 5.5$ denoted as –) forest types.

i	canopy layer	$w_i (+, -)$	$z_i^* (+, -)$	a_{i1}	a_{i2}
T	top	0.75 (0.85,0.65)	40 (42,34)	4.2	4.6
B	bottom	0.25 (0.15,0.35)	13 (8,13)	2.3	1.1

[Title Page](#)

[Abstract](#)

[Introduction](#)

[Conclusions](#)

[References](#)

[Tables](#)

[Figures](#)

◀

▶

◀

▶

[Back](#)

[Close](#)

[Full Screen / Esc](#)

[Print Version](#)

[Interactive Discussion](#)

A coupled model of carbon-water exchange of the Amazon rain forest

E. Simon et al.

Table 5. Leaf optical parameters as recommended by [Leuning et al. \(1995\)](#) and derived by fitting predicted canopy albedo to observations (see Fig. 7).

Parameter	recommended	mean	wet season	dry season
scaling	1.00	0.66	0.60	0.75
σ_{IV}	0.2	0.132	0.120	0.150
σ_{IN}	0.8	0.528	0.480	0.600
ρ_{cdV}	0.057	0.038	0.034	0.043
ρ_{cdN}	0.389	0.257	0.233	0.293
albedo	0.232	0.130	0.1180	0.151



A coupled model of carbon-water exchange of the Amazon rain forest

E. Simon et al.

Table 6. Assessed uncertainties of model key parameters and resulting relative variability of sensible and latent heat flux ($var(H)$) and $var(LE)$, respectively) and of net ecosystem exchange of CO_2 ($var(NEE)$) calculated by the CANVEG model for two mean diurnal circles with wet and dry season environmental conditions, observed at the Jaru site in 1999.

Model parameter (derived mean value)	inferred range (units)	Reference	$var(H)$	$var(LE)$	$var(NEE)$
Mean Canopy structure Λ_z (LAI=6.0)	dense-open	Table 4	104-92%	101-99%	102-96%
Albedo parameter scaling for ρ_c, σ_l (66)	60-75 (%)	Table 5	97-102%	99-100%	101-99%
Photosynthetic capacity $v_{cmax0hc}$ (50)	70-40 ($\mu\text{mol m}^{-2} \text{s}^{-1}$)	Fig. 9	99-103%	101-97%	105-94%
Leaf nitrogen optimization k_N (0.2)	0.0-1.0 (-)	Fig. 9	100-118%	99-79%	101-66%
Light use efficiency α (0.15) and ...	0.2-0.1 (-)	Fig. 12	95-111%	114-78%	126-66%
... shape parameter of light response θ (0.9)	0.95-0.8 (-)				
$g_s - A_n$ correlation coefficient a_A (10)	15-5 (-)	Fig. 13	88-125%	122-59%	107-78%

[Title Page](#)

[Abstract](#)

[Introduction](#)

[Conclusions](#)

[References](#)

[Tables](#)

[Figures](#)

◀

▶

◀

▶

[Back](#)

[Close](#)

[Full Screen / Esc](#)

[Print Version](#)

[Interactive Discussion](#)

Table 7. Photosynthesis and stomatal conductance model parameters. Marked values are taken from ^{*}Leuning et al. (1995) and [†]Harley et al. (1992). Values in brackets are derived from leaf level gas exchange measurements (see Sect. 2.2 for further explanations).

Parameter	Value (optimized)	Unit
a_A	10	[-]
g_{s0}	0.01	[mol m ⁻² s ⁻¹]
D_{s0}	15	[hPa]
$V_{cmax0hc}$	50	[μmol m ⁻² s ⁻¹]
k_N	0.2	[-]
T_{s0}	298.15	[K]
J_{max0}	$2.1V_{cmax0}$	[μmol m ⁻² s ⁻¹]
R_{d0}	$0.01V_{cmax0}$	[μmol m ⁻² s ⁻¹]
o_i	210	[mmol mol ⁻¹]
α	0.2* (0.15)	[mol e mol ⁻¹ quanta]
θ	0.9*	[-]
K_{c0}	302*	[μmol ⁻¹]
K_{o0}	256*	[mmol ⁻¹]
H_{Kc}	59.4 [†]	[kJ mol ⁻¹]
H_{Ko}	36 [†]	[kJ mol ⁻¹]
H_{Rd}	53 [†]	[kJ mol ⁻¹]
H_{VV}	116.3 [†]	[kJ mol ⁻¹]
H_{dV}	202.9 [†]	[kJ mol ⁻¹]
H_{vJ}	79.5 [†] (108)	[kJ mol ⁻¹]
H_{dJ}	201 [†]	[kJ mol ⁻¹]
S_v	0.65 [†]	[kJ mol ⁻¹]
S_j	0.65 [†] (0.66)	[kJ mol ⁻¹]
γ_0	34.6*	[μmol mol ⁻¹]
γ_1	0.0451*	[-]
γ_2	0.000347*	[-]

A coupled model of carbon-water exchange of the Amazon rain forest

E. Simon et al.

[Title Page](#)

[Abstract](#)

[Introduction](#)

[Conclusions](#)

[References](#)

[Tables](#)

[Figures](#)

◀

▶

◀

▶

[Back](#)

[Close](#)

[Full Screen / Esc](#)

[Print Version](#)

[Interactive Discussion](#)

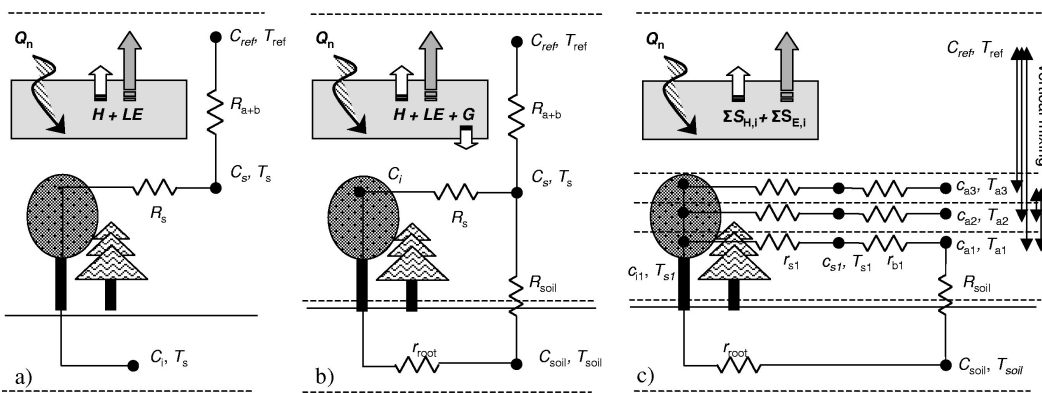


Fig. 1. Calculation of the surface energy balance in three canopy parameterization schemes with increasing complexity: **(a)** Single-layer scheme assuming $T_{soil}=T_s$ with $Q_n=H+LE$. **(b)** Two-layer scheme (soil + big leaf) with $Q_n=H+LE+G$. **(c)** Multi-layer CANVEG scheme (soil + 3 vegetation layers + 1 layer above the canopy) with $Q_n=\sum_i S_{H,i}+S_{LE,i}$. Symbols represent temperature of the soil (T_{soil}), the canopy air (T_a), the foliage (T_s), and the air above the canopy (T_{ref}), available net radiation (Q_n), sensible (H) and latent (LE) heat, the soil heat flux (G), and the stomatal (r_s), leaf boundary-layer (r_b), aerodynamic (r_a), bulk soil surface (r_{soil}) and root (r_{root}) resistance (see also [Garrat, 1992](#)).

A coupled model of carbon-water exchange of the Amazon rain forest

E. Simon et al.

[Title Page](#)

[Abstract](#)

[Introduction](#)

[Conclusions](#)

[References](#)

[Tables](#)

[Figures](#)

◀

▶

◀

▶

[Back](#)

[Close](#)

[Full Screen / Esc](#)

[Print Version](#)

[Interactive Discussion](#)

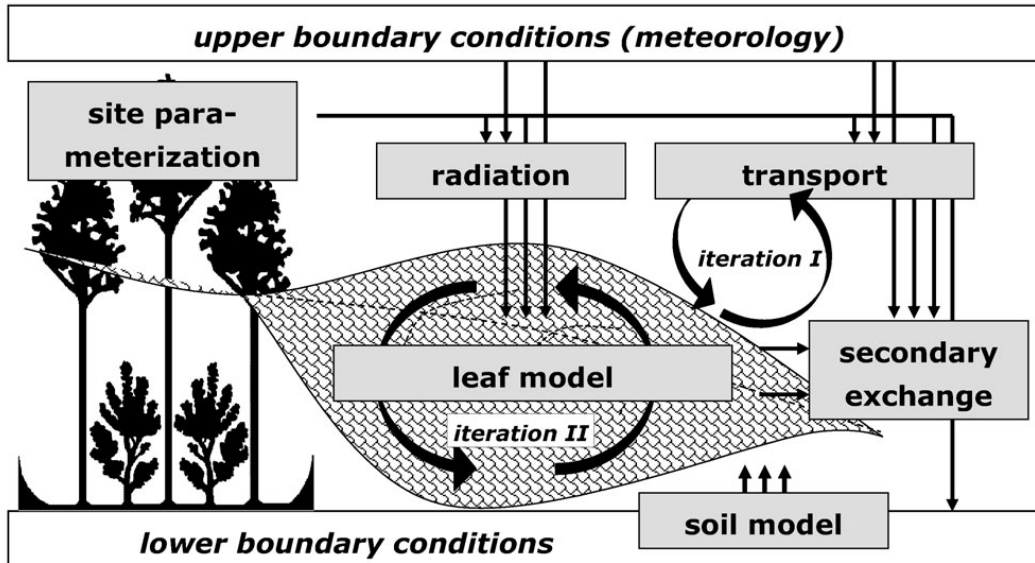


Fig. 2. Sub-models of the modified CANVEG scheme. The two iteration loops I and II indicate the numerical approach to solve the turbulent exchange and the leaf energy balance, respectively.

A coupled model of carbon-water exchange of the Amazon rain forest

E. Simon et al.

[Title Page](#)

[Abstract](#)

[Introduction](#)

[Conclusions](#)

[References](#)

[Tables](#)

[Figures](#)

[◀](#)

[▶](#)

[◀](#)

[▶](#)

[Back](#)

[Close](#)

[Full Screen / Esc](#)

[Print Version](#)

[Interactive Discussion](#)

A coupled model of carbon-water exchange of the Amazon rain forest

E. Simon et al.

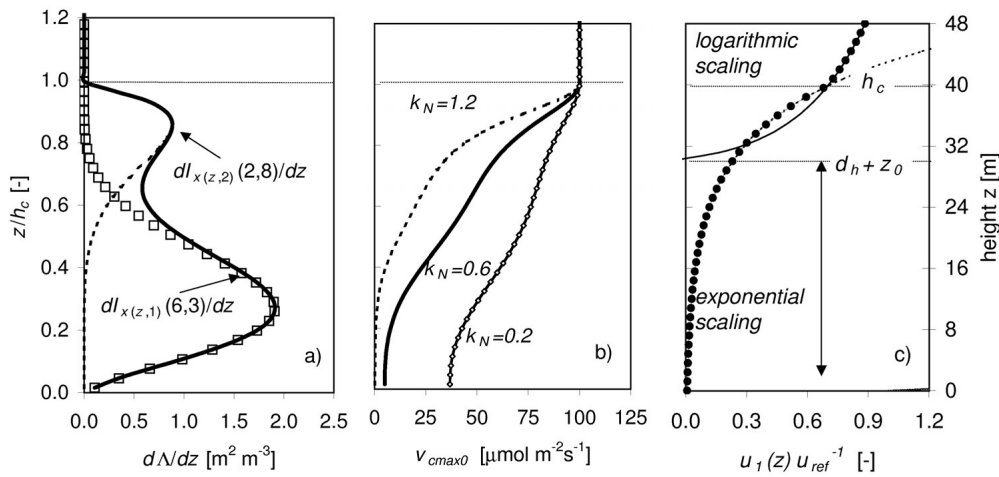


Fig. 3. Site specific profile parameterizations (examples). **(a)** The leaf area density profile ($d\Lambda(z)/dz$), implemented as the sum of two beta distributions (solid line) with an upper (dashed line) and lower (open squares) canopy maximum ($\text{LAI}=1$, lower maximum weight $w_1=0.75$). **(b)** Corresponding light acclimation of leaf biochemistry using different values of extinction (k_N). **(c)** Logarithmic (above canopy, solid line), exponential (below h_c , dashed line) and combined (closed circles) scaling of horizontal wind speed ($u_1(z)$). h_c , z_0 and d_h are the canopy height, roughness length and zero length displacement height, respectively. At $z_0 + d_h$, the logarithmic profiles crosses zero.

- [Title Page](#)
- [Abstract](#) [Introduction](#)
- [Conclusions](#) [References](#)
- [Tables](#) [Figures](#)
- [◀](#) [▶](#)
- [◀](#) [▶](#)
- [Back](#) [Close](#)
- [Full Screen / Esc](#)
- [Print Version](#)
- [Interactive Discussion](#)

A coupled model of carbon-water exchange of the Amazon rain forest

E. Simon et al.

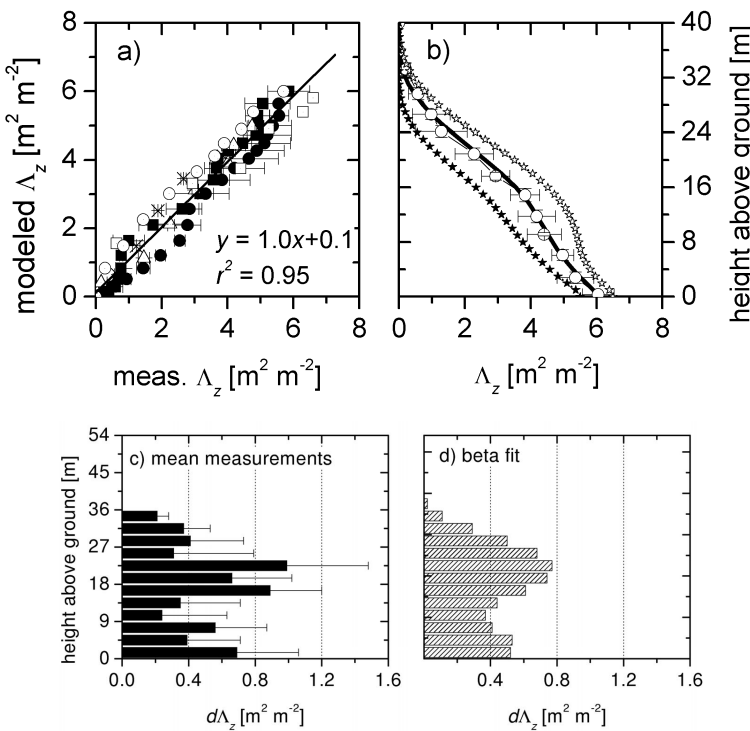


Fig. 4. Parameterization of canopy structure and accumulated leaf area Λ_z . **(a)** Model comparison with field data of Roberts et al. (1993) (open squares) and McWilliam et al. (1993) (open circles), and measurements made at the towers ZF2-K34 (open triangles), ZF2-C14 (stars) RBJ-A (closed squares) and RBJ-B (closed circles, see Table 2). **(b)** Observed accumulated leaf area (Λ_z) for averaged 3 m height intervals (open circles with standard deviations) and predicted for a mean (solid line), dense (open stars) and open (closed stars) forest type. **(c)** Mean observed and **(d)** predicted differential leaf area for 3 m height intervals.

- [Title Page](#)
- [Abstract](#) [Introduction](#)
- [Conclusions](#) [References](#)
- [Tables](#) [Figures](#)
- [◀](#) [▶](#)
- [◀](#) [▶](#)
- [Back](#) [Close](#)
- [Full Screen / Esc](#)
- [Print Version](#)
- [Interactive Discussion](#)

A coupled model of carbon-water exchange of the Amazon rain forest

E. Simon et al.

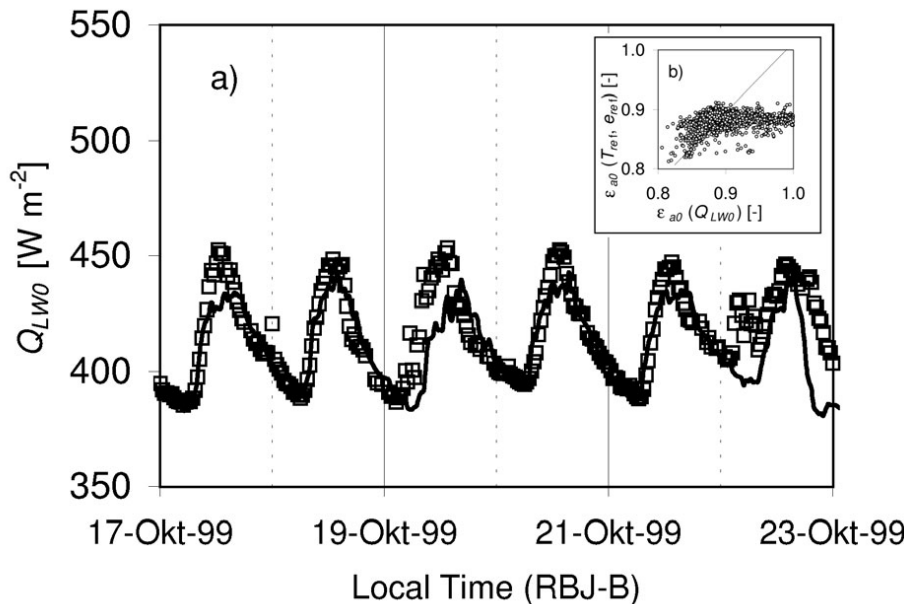


Fig. 5. Observed and predicted Atmospheric emissivity (ϵ_{a0}) and incoming long-wave radiation (Q_{LW0}) at the tower RBJ-B for a one week period. **(a)** Measured (open squares) and predicted time series (solid line) for Q_{LW0} . **(b)** $\epsilon_{a0}(T_{ref}, e_{ref})$ plotted against $\epsilon_{a0}(Q_{LW0})$ (parameterized versus observed atmospheric emissivity, respectively).

- [Title Page](#)
- [Abstract](#) [Introduction](#)
- [Conclusions](#) [References](#)
- [Tables](#) [Figures](#)
- [◀](#) [▶](#)
- [◀](#) [▶](#)
- [Back](#) [Close](#)
- [Full Screen / Esc](#)
- [Print Version](#)
- [Interactive Discussion](#)

A coupled model of carbon-water exchange of the Amazon rain forest

E. Simon et al.

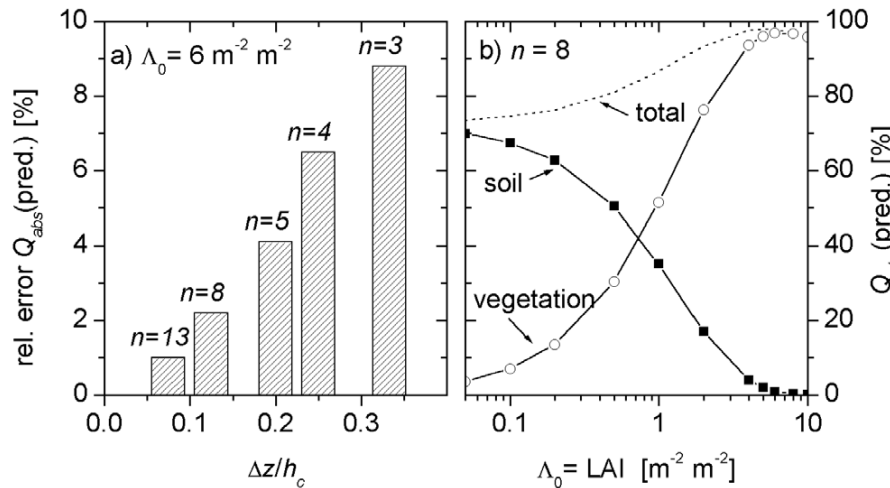


Fig. 6. Absorbed radiation (Q_{abs}) and albedo in relation to the number of canopy layers, leaf area index, and leaf optical parameters for a canopy with black leaves (no reflectance and transmittance) at midday and clear sky conditions with a diffusive fraction $f_{d0}=0.2$. **(a)** Relative error of predicted absorbed radiation in relation to the number (n) and thickness ($\Delta z/h_c$) of canopy layers (total leaf area index $\Lambda_0=6$). **(b)** Predicted total (dotted line), soil (line with filled squares), and vegetation (line with open circles) fractions of absorbed radiation plotted against LAI ($n=8$, $\Delta z=4$ m=0.125 z/h_c).

- [Title Page](#)
- [Abstract](#) [Introduction](#)
- [Conclusions](#) [References](#)
- [Tables](#) [Figures](#)
- [◀](#) [▶](#)
- [◀](#) [▶](#)
- [Back](#) [Close](#)
- [Full Screen / Esc](#)
- [Print Version](#)
- [Interactive Discussion](#)

A coupled model of carbon-water exchange of the Amazon rain forest

E. Simon et al.

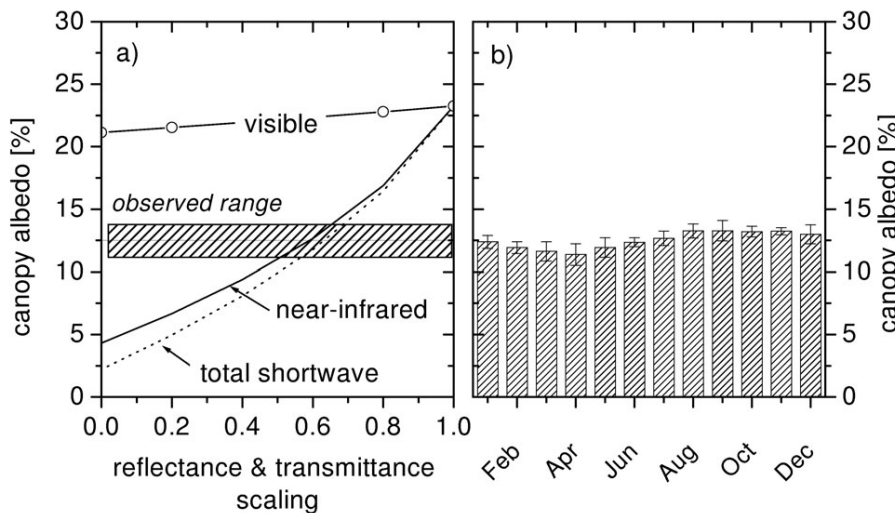


Fig. 7. (a) Observed (hatched box) and predicted canopy albedo at noon time for clear sky conditions ($f_{d0}=0.2$) as a function of relative canopy reflectance and transmittance (1.0 = recommended parameter values, 0.0 = black leaves) for visible (line with open circles), near-infrared (solid line) and total short-wave radiation (dotted line). (b) Annual cycle of canopy albedo as observed at the Jaru site and a second site near Manaus (Reserva Duke) in 1991–1993 (Culf et al., 1995, 1996). Mean and standard deviations of monthly values for both sites are shown ($r^2=0.87$).

- [Title Page](#)
- [Abstract](#) [Introduction](#)
- [Conclusions](#) [References](#)
- [Tables](#) [Figures](#)
- [◀](#) [▶](#)
- [◀](#) [▶](#)
- [Back](#) [Close](#)
- [Full Screen / Esc](#)
- [Print Version](#)
- [Interactive Discussion](#)

A coupled model of carbon-water exchange of the Amazon rain forest

E. Simon et al.

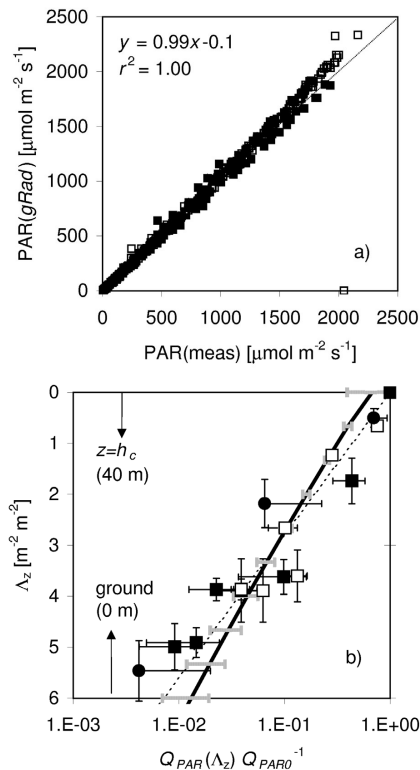


Fig. 8. (a) Incoming PAR (Q_{PAR0}) derived from Eqs. (5)–(6) and observed at towers RBJ-A (closed squares), RBJ-B (closed circles), and ZF2-K34 (open squares). (b) Profiles of mean ratios $Q_{PAR}(\Lambda_z)/Q_{PAR0}$. Observed values at towers ZF2-C14 (open squares), RBJ-A in '92/'93 (closed squares) and RBJ-A in 1999 (closed circles, only positive error bars) and predictions of the two-leaf radiation absorption model constrained with observed meteorology at RBJ-A in October 1999 (solid line with standard deviations). The dotted line represents the exponential fit $y = \exp^{-ax}$, $a=0.82$.

Title Page	
Abstract	Introduction
Conclusions	References
Tables	Figures
◀	▶
◀	▶
Back	Close
Full Screen / Esc	
Print Version	
Interactive Discussion	

A coupled model of carbon-water exchange of the Amazon rain forest

E. Simon et al.

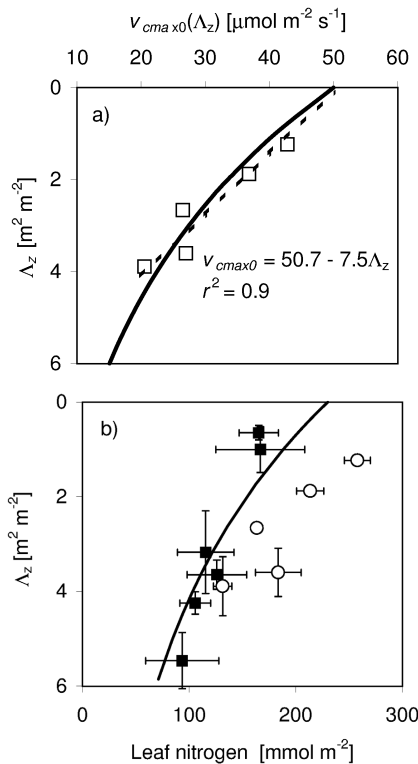


Fig. 9. (a) Relation between accumulated leaf area Λ_z (see Sect. 3.1) and v_{cmax0} (Carswell et al., 2000) observed at the Cuieiras site. The solid and dotted lines represent exponential ($k_N=0.2$) and linear relationships, respectively. (b) Leaf nitrogen concentration c_N at different canopy positions observed at the Cuieiras site (open circles) by Carswell et al. (2000) and observed at the Jaru site (closed squares) by Lloyd et al. (1995). The determination of Λ_z is described in Sect. 3.1. The solid line represents the exponential relationship $c_N=c_{N0} \exp(-\Lambda_z k_N)$ with $c_{N0}=230 \text{ mmol m}^{-2}$.

Title Page	
Abstract	Introduction
Conclusions	References
Tables	Figures
◀ ▶	
◀	▶
Back	Close
Full Screen / Esc	
Print Version	
Interactive Discussion	

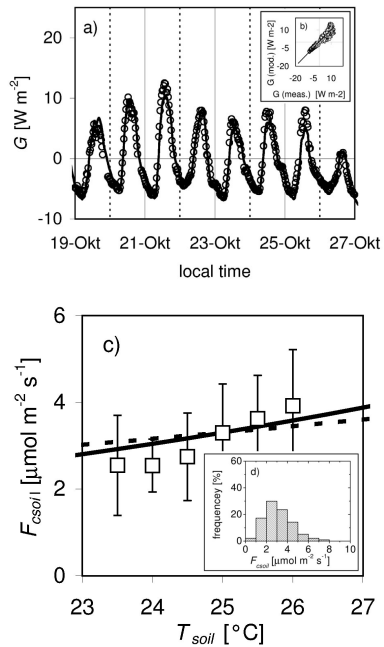


Fig. 10. (a–b) Predicted (open circles) and measured (solid line in (a)) soil heat flux (G) at the tower RBJ-A in 1999 using a constant bulk (0–1 m) soil surface conductance for heat ($1/g_{soilH}=500$ s m⁻¹). The linear fit shown in (b) predicts $y=1.02x + 0.92$ ($r^2=0.92$). (c–d) Parameterization of soil respiration (F_{csoil}) using continuous measurements from three soil chambers and soil temperature (T_{soil}) measured at –0.05 m in 1999 (dry season data from the Jaru site, RBJ-A tower, see Table 2). (c) Mean observations and standard deviations for 0.5°C intervals (open squares) and predictions of Eq. (36) using an optimal $Q_{10}\approx 1.6$ (dashed line) and $Q_{10}\approx 2.3$ (solid line) as derived by Meir et al. (1996) for another site. (d) Frequency distribution of F_{csoil} (total $N=269$).

A coupled model of carbon-water exchange of the Amazon rain forest

E. Simon et al.

[Title Page](#)

[Abstract](#)

[Introduction](#)

[Conclusions](#)

[References](#)

[Tables](#)

[Figures](#)

◀

▶

◀

▶

[Back](#)

[Close](#)

[Full Screen / Esc](#)

[Print Version](#)

[Interactive Discussion](#)

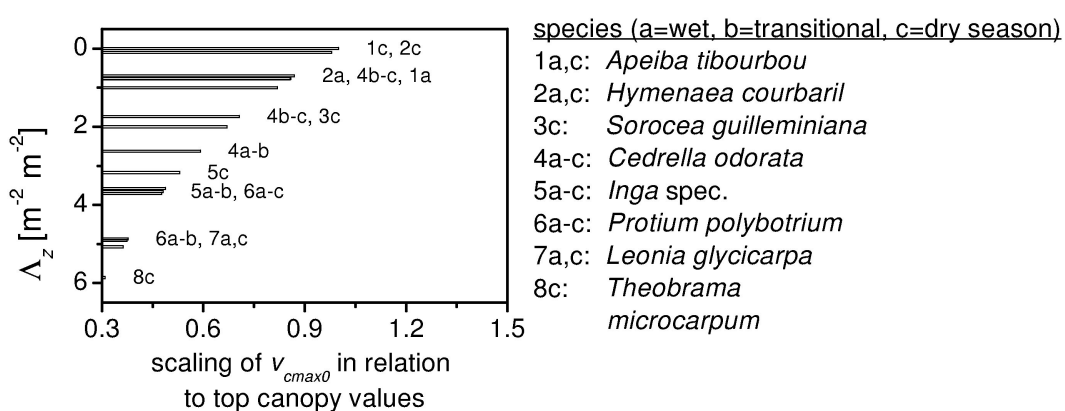


Fig. 11. Scaling of leaf physiology for the evaluation of leaf photosynthesis and stomatal model parameters using gas exchange measurements from 8 tree species made at the Jaru site. Canopy position (Λ_z) and scaling of maximum carboxylation rate (v_{cmax0}) in relation to top canopy values. Measurements for species 1–8 have been made during the late wet (1–8a), early dry (1–8b) and late dry (1–8c) season. The measurement protocol for species 1–3 is described by Kuhn et al. (2002) and Kuhn et al. (2004) whereas measurements for species 4–8 are described by McWilliam et al. (1996).

A coupled model of carbon-water exchange of the Amazon rain forest

E. Simon et al.

[Title Page](#)

[Abstract](#)

[Introduction](#)

[Conclusions](#)

[References](#)

[Tables](#)

[Figures](#)

◀

▶

◀

▶

[Back](#)

[Close](#)

[Full Screen / Esc](#)

[Print Version](#)

[Interactive Discussion](#)

A coupled model of carbon-water exchange of the Amazon rain forest

E. Simon et al.

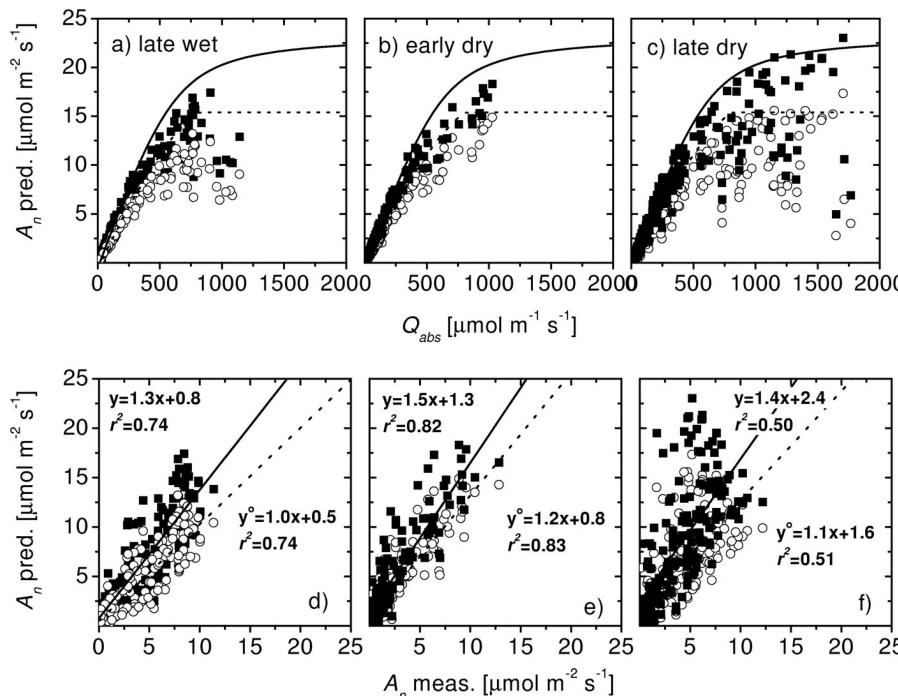


Fig. 12. Light response and comparison of observed and predicted net assimilation (A_n) for different seasonal conditions (late wet: (a), (d); early dry: (b), (e); late dry season: (c), (f)). Measurements are compiled in Table 2 and Fig. 11. (a–c) Light response predicted by the photosynthesis model constrained with observed values of T_s , Q_{PAR} , C_i and parameterized with recommended (closed squares) and optimized (open circles) values for the activation energy and entropy of J_{max} , and the light use efficiency. Dashed and solid lines show the predicted light response for standard conditions ($v_{cmax0} = v_{cmax0hc}$, $C_i = 320 \mu\text{mol mol}^{-1}$ and $T_s = 302 \text{ K}$) using recommended and optimized parameter values, respectively. (d–f) Scatter plot for predicted and observed A_n (same symbols as in a–c). Regression lines y and y' are given for common and optimized parameter values, respectively.

A coupled model of carbon-water exchange of the Amazon rain forest

E. Simon et al.

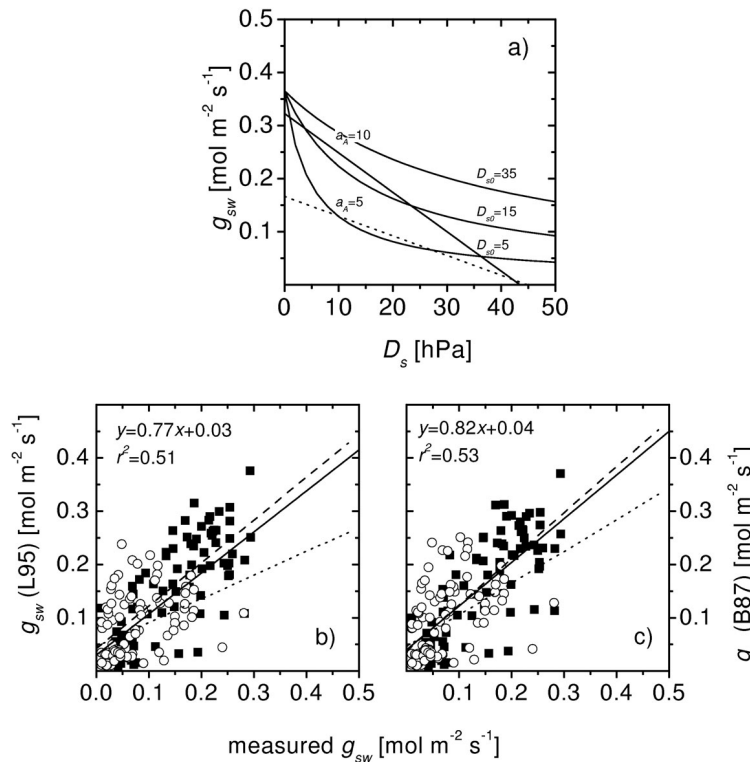


Fig. 13. (a) g_s -Model sensitivity to stomatal parameters. (a) Response to water vapor pressure deficit at the leaf surface (D_s). Predicted slopes for the B87 model (Ball et al., 1987) using $a_A=10$ and $a_A=5$ (dotted line) and predicted curves for the L95 model (Leuning, 1995) using different values for D_{so} ($a_A=10$). Constraining parameters are set to $A_n=10 \mu\text{mol m}^{-2} \text{s}^{-1}$ and $C_s=320 \mu\text{mol mol}^{-1}$. (b–c) Scatter plot of measured and predicted g_{sw} for wet (closed squares; dashed line represents linear fit) and dry (open circles; dotted line represents linear fit) season conditions using the L95 (b) and the B87 model (c). Linear fits for all data are represented by the solid lines.

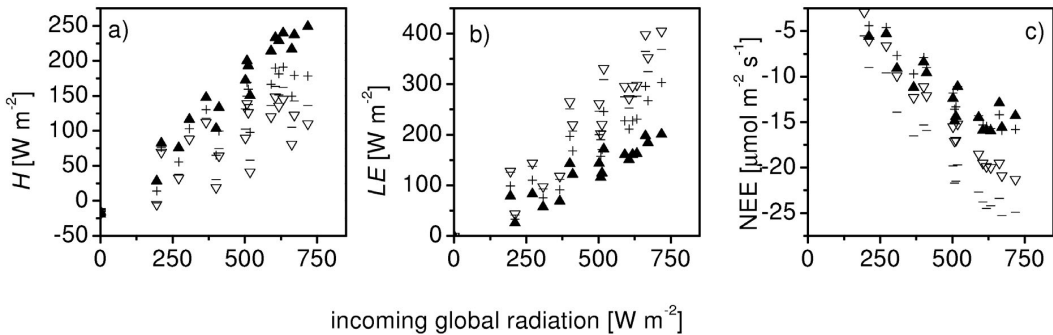


Fig. 14. Predicted canopy fluxes of sensible heat (H), latent heat (LE) and CO_2 (NEE) plotted against incoming global radiation using an increased (+) or decreased (-) stomatal parameter a_A (see Table 6 line 7) and increased (closed upward triangle) or decreased (open downward triangle) photosynthesis parameters α and θ (see line 5–6 in Table 6).

A coupled model of carbon-water exchange of the Amazon rain forest

E. Simon et al.

[Title Page](#)

[Abstract](#)

[Introduction](#)

[Conclusions](#)

[References](#)

[Tables](#)

[Figures](#)

◀

▶

◀

▶

[Back](#)

[Close](#)

[Full Screen / Esc](#)

[Print Version](#)

[Interactive Discussion](#)